

Supporting Information

Efficient Alkene Hydrosilation with Bis(8-quinolyl)phosphine (NPN) Nickel Catalysts.

The Dominant Role of Silyl- over Hydrido-Nickel Catalytic Intermediates

Jian Yang,^a Veronica Postils,^{b,c,d} Michael I. Lipschutz,^a Meg Fasulo,^a Christophe Raynaud,^b
Eric Clot,^b Odile Eisenstein^{*,b,e} and T. Don Tilley^{*,a}

^aDepartment of Chemistry, University of California, Berkeley, California 94720.

^bICGM, Université de Montpellier, CNRS, ENSCM, Montpellier, France.

^cInstitut de Química Computacional i Catàlisi (IQCC) and Departament de Química, Universitat de Girona, Campus Montilivi, 17071, Girona, Spain..

^dKimika Fakultatea, Euskal Herriko Unibertsitatea, PK 1072, 20080, Donostia, Spain

^eHylleraas Centre for Quantum Molecular Sciences, Department of Chemistry, University of Oslo, P.O. Box 1033, Blindern, N-0315, Oslo, Norway

Contents:

EXPERIMENTAL SECTION

(1) Representative Synthetic Procedures:	S-2
(2) Characterization of Hydrosilylation Products:	S-7
(3) References:	S-8

COMPUTATIONAL SECTION

(1) Full Computational Details and associated references.....	S-9
(2) Microkinetic Modeling: Figures S1-S3.....	S-10
(3) Energetic data of the optimized Structures and Profiles:	S-13
Isolated reagents	S-13
Formation of the (NPN)Ni-H ⁺ catalyst Figure S4.....	S-14
Cycle with the (NPN)Ni-H ⁺ catalyst Figure S5.....	S-16
Cycle with the (NPN)Ni-Silyl ⁺ catalyst Figure S6.....	S-21
[(NPN)Ni-H] ⁺ – [(NPN)Ni-Silyl] ⁺ interconversion mediated by a silane moiety ...Figure S7.....	S-27
Structural variety and multiple pathways...Figure S8.....	S-28
(4) NBO analysis of TSB2.....	S-29
(5) Spin-State study.....	S-30

EXPERIMENTAL SECTION

(1) Representative Synthetic Procedures

General considerations.

All manipulations were carried out using Schlenk techniques under a purified N₂ atmosphere or in a Vacuum Atmospheres drybox. Solvents were distilled under N₂ from appropriate drying agents and stored in Straus flasks. Benzene-d₆ was dried by vacuum distillation from Na/K alloy. Silanes, olefin substrates, 1,2-dichlorobenzene and bromobenzene-d₅ were dried over 4 Å molecular sieves or CaH₂, and stored under N₂. Dichloromethane-d₂ was dried with CaH₂ and vacuum transferred into a sealed flask. All other reagents were purchased from Aldrich, Strem, or Gelest, and used as received. 8-bromoquinoline¹ was prepared according to literature procedures. NMR spectra were recorded on Bruker AV-600, DRX-500, AV-500, AVB-400, AVQ-400 and AV-300 spectrometers at room temperature. ¹H NMR spectra were referenced to residual protio solvent peaks (δ 7.16 for C₆D₆, δ 5.32 for CD₂Cl₂, δ 7.03 (4-H) for C₆D₅Br, δ 7.4 (3-H) for o-C₆H₄Cl₂). ¹³C{¹H} NMR spectra were referenced to solvent resonance (δ 128.4 for C₆D₆, δ 54.0 for CD₂Cl₂, δ 122.5 (ipso C) for C₆D₅Br, δ 127.68 (4-C) for o-C₆H₄Cl₂). ³¹P{¹H} NMR chemical shifts were referenced to an external H₃PO₄ standard. Elemental analyses were carried out by the College of Chemistry Microanalytical Laboratory at the University of California, Berkeley. GC-MS analysis was performed on an Agilent Technologies 6890N GC system with an HP-5MS column.

Synthesis of Bis(8-quinolyl)(dimethylamino)phosphine (NMe₂-NPN).

N-butyllithium (1.6 M in hexanes, 4 mL, 6.4 mmol) was added dropwise to a stirred solution of 8-bromoquinoline (1.23 g, 5.92 mmol) in THF (40 mL) at -78 °C. The mixture was stirred for 15 min at this temperature before Me₂NPCl₂ (neat, 0.33 mL, 420 mg, 2.88 mmol) was added via syringe. The reaction mixture was stirred for another 10 min at -78 °C before it was allowed to warm to room temperature; stirring was continued for 18 h. All of the volatile material was removed in vacuo and toluene (35 mL) was added. The yellow slurry was stirred at room temperature for 20 min and then filtered. The yellow extract was concentrated to about 20 mL and filtered. The filtrate was further concentrated to about 10 mL and stored at -35 °C for 2 d. The product was obtained as a pale-yellow solid in 35% yield (330 mg, 1.0 mmol) and exhibited > 95% purity by NMR. It was used without further purification. ¹H NMR (C₆D₆, 600.13 MHz): δ 8.62 (m, 2H), 7.54 (m, 2H), 7.39 (m, 2H), 7.17 (m, 2H), 6.72 (m, 2H), 2.86 (d, J = 9 Hz). ¹³C{¹H} NMR (CD₂Cl₂, 150.92 MHz): δ 150.20 (d, J = 18 Hz), 149.81, 140.96 (d, J = 17 Hz), 136.65, 133.58, 128.58, 128.45, 126.88, 121.60, 43.71 (d, J = 17 Hz). ³¹P{¹H} NMR (C₆D₆, 242.95 MHz): δ 54.5. GC-MS m/z 331 (M⁺), 288, 159. Anal. Calcd. (%) for C₂₀H₁₈N₃P (331.35): C, 72.49, H, 5.47, N, 12.68. Found: C, 72.25, H, 5.55, N, 12.19.

Synthesis of Bis(8-quinolyl)(3,5-di-tert-butylphenoxy)phosphine ($\text{Ar}^{\text{tBu}}\text{O-NPN}$, **1**).

A mixture of **1** (600 mg, 1.81 mmol) and 3,5-di-tert-butylphenol (370 mg, 1.79 mmol) in toluene (15 mL) was refluxed under N_2 for 6 h (bath temperature was 125 °C). All volatile materials were removed in vacuo. Benzene (8 mL) and hexanes (4 mL) were added and the mixture was filtered through Celite[®] and a glass fiber filter to give a yellow solution. The volatile components were removed in vacuo. The residue was washed with cold hexanes and dried in vacuo to give the product as a light-yellow solid (680 mg, 1.38 mmol, 77%). ^1H NMR (C_6D_6 , 499.92 MHz): δ 8.59 (m, 2H), 8.06 (m, 2H), 7.71 (m, 2H), 7.46 (m, 2H), 7.36 (m, 2H), 7.28 (m, 1H), 7.13 (m, 2H), 6.66 (m, 2H), 1.30 (s, 18 H). $^{13}\text{C}\{^1\text{H}\}$ NMR (CD_2Cl_2 , 150.92 MHz): δ 158.50 (d, $J = 12$ Hz), 152.73, 150.23 (d, $J = 1.5$ Hz), 149.88 (d, $J = 20$ Hz), 141.31 (d, $J = 23$ Hz), 136.70 (d, $J = 1.5$ Hz), 132.97 (d, $J = 1.5$ Hz), 129.94, 128.59, 127.18, 121.96, 116.77, 114.13 (d, $J = 11$ Hz), 35.45, 31.79. $^{31}\text{P}\{^1\text{H}\}$ NMR (C_6D_6 , 242.95 MHz): δ 98.0. Anal. Calcd. (%) for $\text{C}_{32}\text{H}_{33}\text{N}_2\text{OP}$ (492.59): C, 78.02, H, 6.75, N, 5.69. Found: C, 77.68, H, 6.69, N, 5.52.

Synthesis of $\text{Ar}^{\text{tBu}}\text{O-NPN})\text{NiCl}_2$ (**2**).

A solution of **1** (500 mg, 1.02 mmol) in CH_2Cl_2 (4 mL) was added to a stirring slurry of $\text{NiCl}_2(\text{DME})$ (200 mg, 0.91 mmol) in CH_2Cl_2 (10 mL). The reaction mixture was allowed to stir at room temperature for 1 d. All volatile materials were removed in vacuo. The residue was washed with diethyl ether (2 mL \times 3) and hexanes (8 mL \times 2), and dried in vacuo to give the product as a light brown solid (340 mg, 0.55 mmol, 60%). The ^1H NMR spectrum of **2** was not obtained due to the poor solubility of **2** in a range of organic solvents, including dichloromethane. Anal. Calcd. (%) for $\text{C}_{32}\text{H}_{33}\text{N}_2\text{OPNiCl}_2$ (622.19): C, 61.77, H, 5.35, N, 4.50. Found: C, 61.80, H, 5.43, N, 4.48.

Synthesis of $\{(\text{Ar}^{\text{tBu}}\text{O-NPN})\text{Ni}(\mu\text{-Cl})\}_2[\text{B}(\text{C}_6\text{F}_5)_4]_2$ (**3a**).

(A) Synthesis and Isolation of **3a** from **2** and $\text{Li}(\text{OEt})_3\text{B}(\text{C}_6\text{F}_5)_4$: A solution of $\text{Li}(\text{OEt})_3\text{B}(\text{C}_6\text{F}_5)_4$ (180 mg, 0.198 mmol) in $\text{C}_6\text{H}_5\text{F}$ (4 mL) was added dropwise to a stirring slurry of **2** (114 mg, 0.183 mmol) in $\text{C}_6\text{H}_5\text{F}$ (6 mL). The resulting solution was stirred at room temperature for 1 d. The reaction mixture was then filtered through Celite[®] and a glass fiber filter, and layered with hexanes (10 mL). At room temperature a dark oil settled out. The oil was separated from the solution, washed with hexanes (3 mL \times 4), and dried in vacuo to give the product as a light green solid (220 mg, 0.087 mmol, 95%). ^1H NMR ($\text{C}_6\text{D}_5\text{Br}$, 600.13 MHz): δ 51.7 (2H), 21.3 (2H), 18.6 (4H), 12.9 (2H), 9.6 (3H), 8.1 (2H) (aryl hydrogens, total 15H), 1.0 (18H, ^tBu). Anal. Calcd. (%) for $\text{C}_{112}\text{H}_{66}\text{N}_4\text{O}_2\text{P}_2\text{Ni}_2\text{Cl}_2\text{B}_2\text{F}_{40}$ (2531.54): C, 53.14, H, 2.63, N, 2.21. Found: C, 53.34, H, 3.02, N, 1.92.

(B) In situ generation of **3a** from **3b** and $\text{Li}(\text{OEt})_3\text{B}(\text{C}_6\text{F}_5)_4$: Bromobenzene- d_5 (0.92 g, 0.6 mL) was added to a solid mixture of **3b** (3.4 mg, 0.0021 mmol, 1 equiv) and $\text{Li}(\text{OEt})_3\text{B}(\text{C}_6\text{F}_5)_4$ (4.0 mg, 0.0044

mmol, 2.1 equiv). The resulting solution was transferred to a J. Young NMR tube. ^1H NMR measurements taken after 1.3 h showed quantitative formation of **3a**.

Synthesis of $[(\text{Ar}^{\text{tBu}}\text{O-NPN})\text{Ni}(\mu\text{-Cl})(\text{SbF}_6)]_2$ (3b**).**

A mixture of **2** (41 mg, 0.066 mmol) and AgSbF_6 (24 mg, 0.070 mmol) in CH_2Cl_2 (4 mL) was stirred at room temperature for 1.5 h. The reaction mixture was filtered through Celite[®] and a glass fiber filter, and pentane (6 mL) was added to precipitate a light green solid. The solid was washed with pentane (4 mL \times 2), and dried in vacuo to give **3b** as a light green powder (43 mg, 0.026 mmol, 79%). ^1H NMR ($\text{C}_6\text{D}_5\text{Br}$, 500.23 MHz): δ 50.2 (2H), 22.4 (2H), 19.2 (2H), 18.0 (2H), 13.1 (2H), 9.0 (3H), 8.1 (2H) (aryl hydrogens, total 15H), 1.0 (18H, ^tBu). Anal. Calcd. (%) for $\text{C}_{64}\text{H}_{66}\text{N}_4\text{O}_2\text{P}_2\text{Ni}_2\text{Cl}_2\text{Sb}_2\text{F}_{12}$ (1644.97): C, 46.73, H, 4.04, N, 3.41. Found: C, 46.39, H, 4.16, N, 3.35. Crystals suitable for X-ray analysis were grown from vapor diffusion of hexanes into a $\text{C}_6\text{H}_5\text{F}$ solution of **3b** at room temperature.

Hydrosilylation of tert-Butylethylene with Ph_2SiH_2 using an in situ Generated Catalyst from **3 and $\text{Li}(\text{OEt})_3\text{B}(\text{C}_6\text{F}_5)_4$.**

Bromobenzene- d_5 (1 g, 0.65 mL) was added to a solid mixture of **2** (5 mg, 0.008 mmol, 1.09 mol%) and $\text{Li}(\text{OEt})_3\text{B}(\text{C}_6\text{F}_5)_4$ (8.3 mg, 0.0091 mmol, 1.23 mol%). The mixture was shaken to allow mixing. After 5 min the solution was added to a mixture of tert-butylethylene (62 mg, 0.737 mmol, 1.0 equiv) and Ph_2SiH_2 (173 mg, 0.939 mmol, 1.27 equiv). The resulting mixture was transferred to a J. Young NMR tube. The reaction went to completion before the first NMR measurement (< 0.6 h).

Hydrosilylation of Cyclopentene with Ph_2SiH_2 using 0.28 mol% **3b (0.56 mol% Ni).**

A solution of **3b** (3.4 mg, 0.00207 mmol, 0.56 mol% Ni) in $\text{C}_6\text{D}_5\text{Br}$ (0.92 g, 0.6 mL) was added to a mixture of cyclopentene (50 mg, 0.737 mmol, 1.0 equiv) and Ph_2SiH_2 (173 mg, 0.939 mmol, 1.27 equiv). The resulting orange solution was transferred to a J. Young NMR tube. The reaction mixture was allowed to stand at room temperature and the reaction progress was monitored by NMR spectroscopy. Hydrosilylation products were identified by ^1H and $^{13}\text{C}\{^1\text{H}\}$ NMR spectroscopies.

General Procedure for the hydrosilylation of alkenes with secondary silanes using **3a.**

A solution in $\text{C}_6\text{D}_5\text{Br}$ containing the alkene (1 equiv), the silane (1.27 equiv) and a known quantity of internal standard (either hexamethylbenzene or tetrakis(trimethylsilyl)silane) was added to a vial containing **3a** (0.28-3.0 mol%). The contents were mixed until all of the solid was dissolved and the solution was transferred to a J-young NMR tube. The reaction mixtures were allowed to stand at room

temperature and the reaction progress was monitored by NMR spectroscopy. The hydrosilation products were identified by ^1H and $^{13}\text{C}\{^1\text{H}\}$ NMR spectroscopies. The yield of products was determined by integration against the internal standard. The reaction mixture was then exposed to air, diluted with hexanes, filtered through a glass fiber filter and analyzed by GC/MS.

General Procedure for the hydrosilation of alkenes with primary and tertiary silanes using **3a.**

A solution in $\text{o-C}_6\text{H}_4\text{Cl}_2$ containing the alkene (1 equiv) and the silane (1.27 equiv) was added to a vial containing **3a** (0.28-3.0 mol%). The contents were mixed until all of the solid was dissolved and the solution was transferred to a J-young NMR tube containing a sealed capillary of C_6D_6 . The reaction mixtures were allowed to stand at room temperature and the reaction progress was monitored by NMR spectroscopy. The hydrosilation products were identified by ^1H and $^{13}\text{C}\{^1\text{H}\}$ NMR spectroscopies. After the reaction had completed, a known quantity of an internal standard (either hexamethylbenzene or tetrakis(trimethylsilyl)silane) was added to the reaction mixture. The yield of products was then determined by integration against this internal standard. The reaction mixture was then exposed to air, diluted with hexanes, filtered through a glass fiber filter and analyzed by GC/MS.

Hydrosilylation of 1-Hexene with Ph_2SiH_2 Catalyzed by **3a without Solvent.**

A mixture of 1-hexene (155 mg, 1.84 mmol, 1.0 equiv) and Ph_2SiH_2 (433 mg, 2.35 mmol, 1.28 equiv) was added to **3a** (5.5 mg, 0.00217 mmol, 0.23 mol% Ni) in a J. Young NMR tube with a sealed capillary tube with C_6D_6 for a NMR lock. The reaction mixture was allowed to stand at room temperature and the reaction progress was monitored by NMR spectroscopy. The hydrosilylation products were identified by ^1H and $^{13}\text{C}\{^1\text{H}\}$ NMR spectroscopies.

Hydrosilylation of tert-Butylethylene with Ph_2SiD_2 Catalyzed by **3a.**

A solution of **3a** (2.2 mg, 0.00087 mmol, 1.05 mol% Ni) in $\text{C}_6\text{D}_5\text{Br}$ (0.94 g, 0.6 mL) was added to a mixture of tert-butylethylene (14 mg, 0.166 mmol, 1.0 equiv) and Ph_2SiD_2 (47 mg, 0.252 mmol, 1.52 equiv). The resulting solution was transferred to a J. Young NMR tube. The reaction mixture was allowed to stand at room temperature and the reaction progress was followed by ^1H and $^{13}\text{C}\{^1\text{H}\}$ NMR spectroscopies. Analysis of the NMR spectra by comparison to $^{13}\text{C}\{^1\text{H}\}$ NMR data of undeuterated $\text{Ph}_2\text{SiHCH}_2\text{CH}_2^t\text{Bu}$ revealed an approximately 1:1.6 ratio of $\text{Ph}_2\text{SiDCHDCH}_2^t\text{Bu}$ and $\text{Ph}_2\text{SiDCH}_2\text{CHD}^t\text{Bu}$. $^{13}\text{C}\{^1\text{H}\}$ NMR ($\text{C}_6\text{D}_5\text{Br}$, 125.72 MHz): $\text{Ph}_2\text{SiDCH}_2\text{CHD}^t\text{Bu}$: δ 38.14 (t, $J_{\text{D,C}} = 19$ Hz), 6.60 (s); $\text{Ph}_2\text{SiDCHDCH}_2^t\text{Bu}$: δ 38.48 (s), 6.35 (t, $J_{\text{D,C}} = 19$ Hz).

(2) Characterization of Hydrosilylation Products³⁻⁵

Ph₂SiHCH₂CH₂^tBu: ¹H NMR (C₆D₅Br, 400.13 MHz): Characteristic chemical shifts of Si-H and alkyl group: δ 5.05 (t, J = 3.6 Hz, Si-H, 1H), 1.42-1.38 (m, 2H), 1.15-1.09 (m, 2H), 0.86 (s, 9H). ¹³C{¹H} NMR (C₆D₅Br, 125.75 MHz): δ 135.38, 134.73, 129.75, 128.26, 38.59, 31.28, 28.96, 6.81. GC-MS: m/z 268 (M⁺), 183, 162, 105.

Ph₂SiH(cyclopentyl): ¹H NMR (C₆D₅Br, 600.13 MHz): Characteristic chemical shifts of Si-H and alkyl group: δ 4.96 (Si-H, 1H), 1.92-1.82 (m, 2H), 1.60-1.42 (m, 7H). ¹³C{¹H} NMR (C₆D₅Br, 125.75 MHz): δ 135.65, 134.71, 129.65, 128.15, 29.44, 27.22, 22.90. GC-MS: Ph₂SiH(cyclopentyl): m/z 252 (M⁺), 183, 105. Ph₂Si(cyclopentyl)₂: m/z 320 (M⁺), 251, 183, 105.

Ph₂SiH(CH₂)₃CH(CH₃)₂: ¹H NMR (C₆D₅Br, 600.13 MHz): δ 7.60-7.59 (m, overlap with Ph₂Si[(CH₂)₃CH(CH₃)₂]₂), 7.30-7.26 (m, overlap with Ph₂Si[(CH₂)₃CH(CH₃)₂]₂), 5.06 (t, J = 3.6 Hz, Si-H, 1H), 1.53-1.46 (m, overlap with Ph₂Si[(CH₂)₃CH(CH₃)₂]₂), 1.28-1.23 (m, overlap with Ph₂Si[(CH₂)₃CH(CH₃)₂]₂), 1.16-1.11 (m, overlap with Ph₂Si[(CH₂)₃CH(CH₃)₂]₂), 0.84 (m, overlap with Ph₂Si[(CH₂)₃CH(CH₃)₂]₂). ¹³C{¹H} NMR (C₆D₅Br, 150.92 MHz): δ 135.37, 134.81, 129.71, 128.23, 42.73, 27.76, 22.82, 22.50, 12.58.

Ph₂Si[(CH₂)₃CH(CH₃)₂]₂: ¹³C{¹H} NMR (C₆D₅Br, 150.92 MHz): δ 136.84, 135.11, 129.30, 128.05, 43.32, 27.62, 22.86, 21.77, 12.98. GC-MS: Ph₂SiH(CH₂)₃CH(CH₃)₂: m/z 267 ((M-H)⁺), 190, 183, 105. Ph₂Si[(CH₂)₃CH(CH₃)₂]₂: m/z 351 ((M-H)⁺), 337, 274, 267, 183, 105.

Ph₂SiH(CH₂)₅CH₃: ¹H NMR (C₆D₅Br, 300.13 MHz): δ 7.61-7.58 (m, overlap with Ph₂Si[(CH₂)₅CH₃]₂), 7.31-7.25 (m, overlap with Ph₂Si[(CH₂)₅CH₃]₂), 5.05 (t, J = 3.6 Hz, Si-H, 1H), 1.51-1.11 (m, overlap with Ph₂Si[(CH₂)₅CH₃]₂), 0.87 (t, J = 7 Hz, overlap with Ph₂Si[(CH₂)₅CH₃]₂). ¹³C{¹H} NMR (C₆D₅Br, 75.48 MHz): δ 135.38, 134.81, 129.70, 128.22, 33.23, 31.77 (overlap with Ph₂Si[(CH₂)₅CH₃]₂), 24.74, 22.95, 14.50 (overlap with Ph₂Si[(CH₂)₅CH₃]₂), 12.51. Ph₂Si[(CH₂)₅CH₃]₂: ¹³C{¹H} NMR (C₆D₅Br, 150.92 MHz): δ 136.84, 135.14, 129.29, 128.05, 33.80, 31.77 (overlap with Ph₂SiH(CH₂)₅CH₃), 24.07, 23.02, 14.50 (overlap with Ph₂SiH(CH₂)₅CH₃), 12.92. GC-MS: Ph₂SiH(CH₂)₅CH₃: m/z 268 (M⁺), 183, 105. Ph₂Si[(CH₂)₅CH₃]₂: m/z 352 (M⁺), 267, 183, 105.

Et₂SiHCH₂CH₂^tBu: ¹H NMR (C₆D₅Br, 400.13 MHz): δ 3.79 (m, Si-H, 1H), 1.24-1.20 (m, 2H), 1.00-0.94 (m, overlap with excess Et₂SiH₂), 0.86 (s, 9H), 0.61-0.50 (m, overlap with excess Et₂SiH₂). ¹³C{¹H} NMR (C₆D₅Br, 100.62 MHz): δ 38.85, 31.24, 28.99, 8.58, 4.93, 3.03. GC-MS: m/z 172 (M⁺), 157, 143, 129, 115.

PhMeSiH(cyclopentyl): ¹H NMR (C₆D₅Br, 499.92 MHz): δ 7.58-7.50 (m), 7.30-7.25 (m), 4.43 (m, Si-H, overlap with excess PhMeSiH₂), 1.77 (m), 1.56-1.41 (m), 1.35 (m), 1.10 (m), 0.30 (d, J = 4 Hz, overlap with excess PhMeSiH₂). ¹³C{¹H} NMR (C₆D₅Br, 125.72 MHz): δ 136.42, 134.79, 129.37, 128.04, 29.25, 28.89, 27.25, 27.22, 23.94, -6.55. GC-MS: m/z 190 (M⁺), 121, 112, 105.

Ph₂MeSi(cyclopentyl): ¹H NMR (o-C₆H₄Cl₂, 600.13 MHz): δ 7.76-7.74 (m, overlap with excess PhMeSiH₂), 7.50-7.48 (m, overlap with excess PhMeSiH₂), 2.02 (m, 2H), 1.73-1.57 (m, 7H), 0.72 (s, 3H). ¹³C{¹H} NMR (o-C₆H₄Cl₂, 150.92 MHz): δ 137.31, 134.89 (overlap with excess Ph₂MeSiH), 129.12, 127.86, 28.70, 27.28, 24.18, -5.96. GC-MS: m/z 266 (M⁺), 197.

Ph₂MeSi(CH₂)₃CH(CH₃)₂: ¹H NMR (o-C₆H₄Cl₂, 600.13 MHz): δ 7.76-7.75 (m, overlap with excess PhMeSiH₂), 7.51-7.48 (m, overlap with excess PhMeSiH₂), 1.71 (septet, J = 6.6 Hz, 1H), 1.64 (m, 2H), 1.43 (m, 2H), 1.27 (m, 2H), 1.04 (d, J = 7.2 Hz, 6H), 0.76 (s, 3H, overlap with excess PhMeSiH₂). ¹³C{¹H} NMR (o-C₆H₄Cl₂, 150.92 MHz): δ 137.58, 134.57, 129.19, 127.96, 43.14, 27.62, 22.67, 21.77, 14.45, -4.35. GC-MS: m/z 267 ((M-CH₃)⁺), 204, 197.

(Me₃SiO)₂MeSi(cyclopentyl): ¹H NMR (o-C₆H₄Cl₂, 600.13 MHz): δ 1.93-1.88 (m, 2H), 1.78-1.72 (m, 2H), 1.70-1.64 (m, 2H), 1.60-1.54 (m, 2H), 1.02 (m, 1H), 0.32 (s, 18H), 0.22 (s, 3H). ¹³C{¹H} NMR (o-C₆H₄Cl₂, 150.92 MHz): δ 27.59, 27.42, 27.12, 2.01, -1.61. GC-MS m/z 290 (M⁺), 275, 221, 207.

Ph₂ClSi(cyclopentyl): ¹H NMR (o-C₆H₄Cl₂, 600.13 MHz): δ 7.86 (m), 7.55-7.50 (m, overlap with excess Ph₂ClSiH), 2.04 (m, 2H), 1.88 (m, 1H), 1.81-1.70 (m, 6H). ¹³C{¹H} NMR (o-C₆H₄Cl₂, 150.92 MHz): δ 134.67, 133.79, 130.45, 128.10, 28.06, 27.18, 25.94. GC-MS: m/z 286 (M⁺), 217, 181.

PhSiH₂(cyclopentyl): ¹H NMR (o-C₆H₄Cl₂, 600.13 MHz): Characteristic chemical shifts of Si-H and alkyl group: δ 4.53 (d, J = 3 Hz, 2H), 2.02 (m, 2H), 1.76 (m, 2H), 1.68 (m, 2H, overlap with other minor side product), 1.57 (m, 2H), 1.41 (m, 1H). ¹³C{¹H} NMR (C₆D₅Br, 150.92 MHz): δ 135.65, 132.72, 129.68, 128.16, 29.90, 27.17, 21.36. GC-MS: m/z 176 (M⁺), 148, 133, 120, 107, 98, 81, 67.

MesSiH₂(cyclopentyl): ¹H NMR (o-C₆H₄Cl₂, 499.92 MHz): Characteristic chemical shifts of Si-H and alkyl group: δ 4.62 (d, 2H), 2.61 (s, 6H), 2.40 (s, 3H), 2.00 (m, 2H), 1.81 (m, 2H), 1.69 (m, 2H), 1.57 (m, 2H), 1.43 (m, 1H). GC-MS: m/z 218 (M⁺), 150, 135, 119, 105.

(3) References

- (1) J. L. Butler and M. Gordon, *J. Heterocycl. Chem.*, 1975, **12**, 1015-1020.
- (2) A. G. Massey and A. J. Park, *J. Organomet. Chem.*, 1964, **2**, 245-250.
- (3) Hydrosilylation with Ph₂SiH₂: (a) T. Takahashi, M. Hasegawa, N. Suzuki, M. Saburi, C. J. Rousset, P. E. Fanwick, E. Negishi, *J. Am. Chem. Soc.* 1991, **113**, 8564; (b) I. Buslov, J. Becouse, S. Mazza, M. Montandon-Clerc and X. Hu *Angew. Chem. Int. Ed.* 2015, **54**, 14523; (c) Z. Zhang, L. Bai and X. Hu, *Chem. Sci.*, 2019, **10**, 3791-3795.
- (4) Hydrosilylation with MesSiH₃: E. Calimano and T. D. Tilley, *J. Am. Chem. Soc.* 2008, **130**, 9226-9227.
- (5) Hydrosilylation with alkoxysilanes: (a) I. Pappas, S. Treacy and P. J. Chirik, *ACS Catal.*, 2016, **6**, 4105-4109. (b) I. Buslov, F. Song and X. Hu, *Angew. Chem. Int. Ed.*, 2016, **55**, 12295-12299.

COMPUTATIONAL SECTION

(1) Full Computational Details and associated references

The optimization was carried with the Gaussian 09 Rev.D.01 package,¹ with the PBE0 functional² including the Grimme correction for dispersion effects (D3 correction, BJ damping)^{3,4} with the Def2-SVP basis set⁵ for all atoms but Ni, which was represented by the SDD quasi relativistic effective core potential (ECP) and associated basis set⁶ completed by a f polarization function (exp. 3.130)⁷ (BS1 level). Single point calculations were carried out with BS2 level. BS2 level is defined as follows. Def2-TZVPP basis set for all atoms⁵ and the SDD quasi-relativistic ECP for Ni. For Ni the basis set associated with the SDD ECP was completed by 2f1g polarization functions.⁸ The solvent effect (1,2 dichlorobenzene) was included with the SMD^{9,10} representation also at a single point level.

The nature of the extrema as minima was confirmed by analytical frequency calculations at the BS1 level. This level was also used for the statistical mechanics calculations of the thermal and entropic effects which were carried out using the rigid rotor/harmonic oscillator approximation at room temperature and 1 atm. The Gibbs energies were calculated at 298.15 K and 1 atm as follows:

$$G^{1,2-\text{dichlorobenzene,PBE0-D3BJ,BS2}} = E^{1,2-\text{dichlorobenzene,PBE0-D3BJ,BS2}} + G_{\text{contribution}}^{\text{gas,PBE0-D3BJ,BS1}}$$

The Gibbs energies, as defined above, were used to discuss the results using the separated (PNP)Ni-H⁺ complex, the cyclopentene and PhSiH₃ as origin of energy. The NBO analysis¹¹ was carried out with NBO6.¹²

Numerous calculations were first carried out with SiH₄ and ethylene to help delineate the essential characteristics of the reaction pathways with models of silane and alkene closer to the experimental systems. Significantly, the multiple pathways involving SiH₄ and ethylene and PhSiH₃ and cyclopentene reveal significant similarities. The results with SiH₄ and ethylene are not reported.

- (1) Gaussian 16, Revision B.01, M. J. Frisch, G. W. Trucks, H. B. Schlegel, G. E. Scuseria, M. A. Robb, J. R. Cheeseman, G. Scalmani, V. Barone, G. A. Petersson, H. Nakatsuji, X. Li, M. Caricato, A. V. Marenich, J. Bloino, B. G. Janesko, R. Gomperts, B. Mennucci, H. P. Hratchian, J. V. Ortiz, A. F. Izmaylov, J. L. Sonnenberg, D. Williams-Young, F. Ding, F. Lipparini, F. Egidi, J. Goings, B. Peng, A. Petrone, T. Henderson, D. Ranasinghe, V. G. Zakrzewski, J. Gao, N. Rega, G. Zheng, W. Liang, H. Hada, M. Ehara, K. Toyota, R. Fukuda, J. Hasegawa, M. Ishida, T. Nakajima, Y. Honda, O. Kitao, H. Nakai, T. Vreven, K. Throssell, J. A. Jr. Montgomery, J. E. Peralta, F. Ogliaro, M. J. Bearpark, J. J. Heyd, E. N. Brothers, K. N. Kudin, V. N. Staroverov, T. A. Keith, R. Kobayashi, J. Normand, K. Raghavachari, A. P. Rendell, J. C. Burant, S. S. Iyengar, J. Tomasi, M. Cossi, J. M. Millam, M. Klene, C. Adamo, R. Cammi, J. W. Ochterski, R. L. Martin, K. Morokuma, O. Farkas, J. B. Foresman and D. J. Fox, Gaussian, Inc., Wallingford CT, 2016. Revision D.01.
- (2) C. Adamo and V. Barone, *J. Chem. Phys.*, 1999, **110**, 6158-6170.
- (3) S. Grimme, J. Antony, S. Ehrlich and H. Krieg, *J. Chem. Phys.*, 2010, **132**, 154104.
- (4) S. Grimme, S. Ehrlich and L. Goerigk, *J. Comput. Chem.*, 2011, **32**, 1456-1465.
- (5) F. Weigend and R. Ahlrichs, *Phys. Chem. Chem. Phys.*, 2005, **7**, 3297-3305.
- (6) M. Dolg, U. Wedig, H. Stoll and H. Preuss, *J. Chem. Phys.*, 1987, **86**, 866-872.
- (7) A. W. Ehlers, M. Böhme, S. Dapprich, A. Gobbi, A. Höllwarth, V. Jonas, K. F. Köhler, R. Stegmann, A. Veldkamp and G. Frenking, *Chem. Phys. Lett.*, 1993, **208**, 111-114.
- (8) J. M. L. Martin and A. Sundermann, *J. Chem. Phys.*, 2001, **114**, 3408-3420.

- (9) A. V. Marenich, C. J. Cramer and D. G. Truhlar, *J. Phys. Chem. B.*, 2009, **113**, 6378-6396.
- (10) J. Tomasi, B. Mennucci and R. Cammi, *Chem. Rev.*, 2005, **105**, 2999-3094.
- (11) A. E. Reed, L. A. Curtiss and F. Weinhold, *Chem. Rev.*, 1988, **88**, 899-926.
- (12) E. D. Glendening, J. K. Badenhop, A. E. Reed, J. E. Carpenter, J. A. Bohmann, C. M. Morales, C. R. Landis and F. Weinhold, Theoretical Chemistry Institute, University of Wisconsin: Madison, WI, 2018; <http://nbo6.chem.wisc.edu/>.

(2) Microkinetic Modeling

The microkinetic model was constructed using the following elementary chemical steps, with the Gibbs energy of reaction and activation taken from the calculations:

Reactants: Cy-ene: cyclopentene; Ni-H: Ni-hydride cationic complex; Ni-Si: Ni-silyl cationic complex.

Products: Cy-ane: cyclopentane; Si-Cy-ane: monosilylcyclopentane; bisSi-Cy-ane or Si₂-Cy-ane: bis-silylcyclopentane.

Intermediates: I, II, VII and VIII intermediates are shown on Figures S5 and S6 in this SI (pages S21 and S26, respectively).

- 1- From Ni-H to Ni-Silyl: $\text{Ni-H} + \text{PhSiH}_3 \rightarrow \text{Ni-Si} + \text{H}_2$ with $\Delta G = -0.6$ and $\Delta G^\ddagger = 6.9$
- 2- Coordination of Cy-ene to Ni-H: $\text{Ni-H} + \text{Cy-ene} \rightarrow \text{I}$ with $\Delta G = -6.9$ and $\Delta G^\ddagger = 5.0$
- 3- Insertion of Cy-ene into Ni-H: $\text{I} \rightarrow \text{II}$ with $\Delta G = -7.0$ and $\Delta G^\ddagger = 4.6$
- 4- Formation of Si-Cy-ane and Ni-H: $\text{II} + \text{PhSiH}_3 \rightarrow \text{Ni-H} + \text{Si-Cy-ane}$ with $\Delta G = -1.3$ and $\Delta G^\ddagger = 18.5$
- 5- Coordination of Cy-ene to Ni Silyl: $\text{Ni-Si} + \text{Cy-ene} \rightarrow \text{VII}$ with $\Delta G = -1.8$ and $\Delta G^\ddagger = 5$
- 6- Insertion of Cy-ene into Ni-Si: $\text{VII} \rightarrow \text{VIII}$ with $\Delta G = 4.2$ and $\Delta G^\ddagger = 6.2$
- 7- Formation of Cy-ane and Ni silyl: $\text{VIII} + \text{PhSiH}_3 \rightarrow \text{Ni-Si} + \text{Si-Cy-ane}$ with $\Delta G = -18.0$ and $\Delta G^\ddagger = 9.8$
- 8- Formation of Cy-ane: $\text{VIII} + \text{PhSiH}_3 \rightarrow \text{Ni-Si} + \text{Cy-ane}$ with $\Delta G = -10.0$ and $\Delta G^\ddagger = 16.1$
- 9- Formation of the bisSi-Cy-ane : $\text{VIII} + \text{PhSiH}_3 \rightarrow \text{Ni-H} + \text{bisSi-Cy-ane}$ with $\Delta G = -6.4$ and $\Delta G^\ddagger = 11.8$

The study was carried out for various ratios of Ni-H/Cy-ene/PhSiH₃.

For a ratio Ni-H: Cy-ene: PhSiH₃ of 1:1:1, the evolution of the various possible products is as indicated in the figure below. The alkane is the major product formed with very little of mono-silyl cyclopentane and none of the bis-silylcyclopentane. The Ni-containing species is essentially Ni-Si growing as Cy-ane is growing. The situation is such that Cy-ene coordinates to Ni-H very easily and forms II along an exoergic process. At this stage no PhSiH₃ has been used. This is a very rapid process that cannot be seen on this time scale. II either forms Cy-ane or Si-Cy-ane but the latter has a barrier of ca. 2.4 kcal mol⁻¹ higher, thus the major formation of Cy-ane.

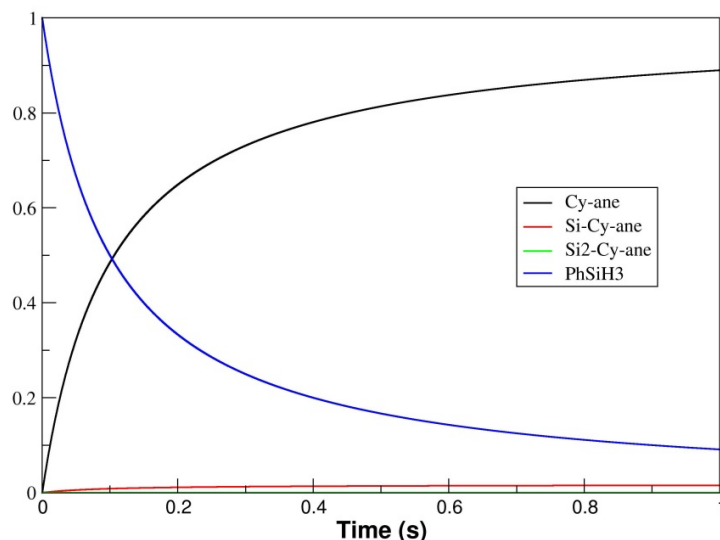


Figure S1: Evolution of the products and the PhSiH_3 silane for the $\text{Ni-H:Cy-ene:PhSiH}_3$ (1:1:1) ratio.

For ratio $\text{Ni-H:Cy-ene:PhSiH}_3$ of 1:10:10 (more realistic of the experimental situation) the situation is totally different as illustrated in the figure below. The mono-silyl cyclopentane is formed almost exclusively and very rapidly. Contrary to the situation above, some bis-silyl cyclopentane is formed, yet in small quantities. The cyclopentane is also formed but as a minor product now.

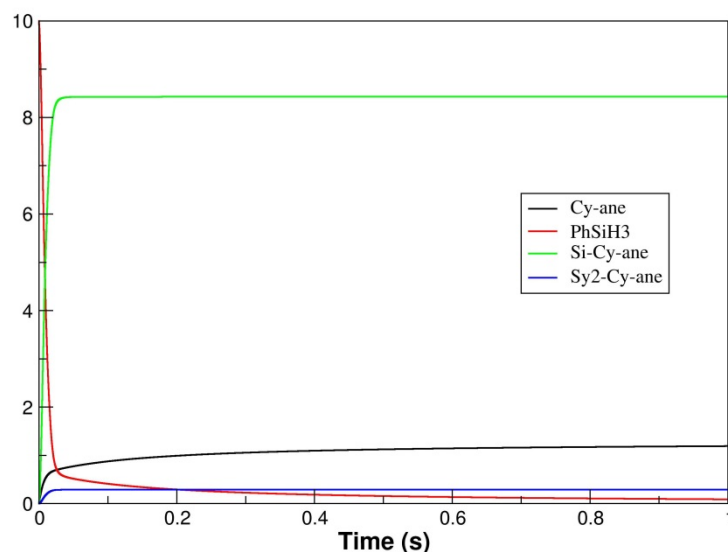


Figure S2: Evolution of the products and the PhSiH_3 silane for the $\text{Ni-H:Cy-ene:PhSiH}_3$ (1:10:10) ratio.

A closer look at the early time of the reaction on the Ni-containing species is shown in the figure below. As in the stoichiometric case, easy coordination to Ni-H followed by alkene insertion into Ni-H forms immediately complex II. Then an equilibrium is installed between II and VII and VII becomes the active catalysts for mono-silane production as illustrated by the steep increase of Si-Cy-ane. Once the silane and the alkene have been consumed, the equilibrium between VII and II no longer exists and II decays as in the stoichiometric case to form alkane and Ni-Si.

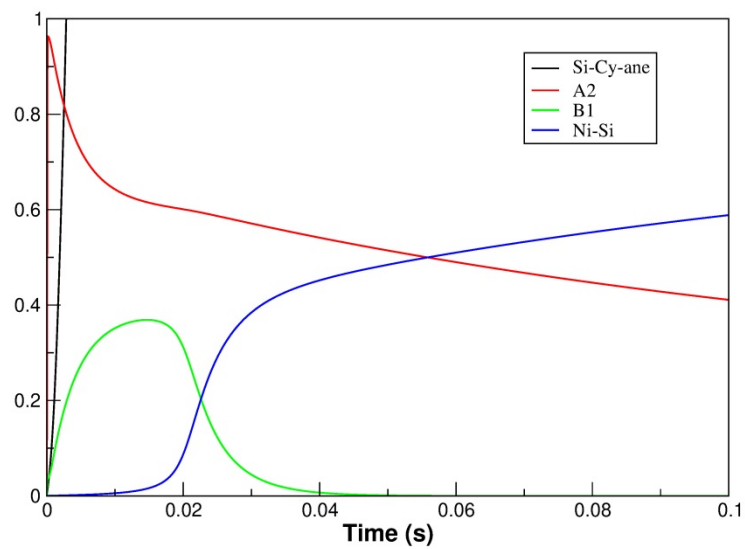


Figure S3: Evolution for the Ni-H:Cy-ene:PhSiH₃ (1:10:10) ratio. In the graphic, A2 refers to II and B1 refers to VII.

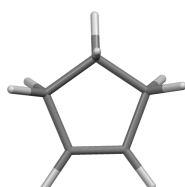
This microkinetic study clearly reinforces the proposal that the catalysis is under the control of the silyl complex.

(3) Energy data of the optimized structures and profiles

The Cartesian coordinates of all computed structures are given in a separate text file in an .xyz format that can be directly read by Mercury. Calculated species and energy profiles below use the same labels as in the .xyz file.

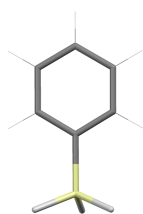
Isolated reagents

Cyclopentene



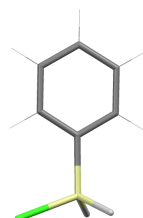
$E_{\text{elec}}^{\text{BS1}}$:	-194.9569345 a.u.
$E_{\text{elec}}^{\text{SMD,BS2}}$:	-195.1721207 a.u.
E_{disp} :	-0.008520285 a.u.
H correc:	0.122618 a.u.
G correc:	0.089785 a.u.
H(total):	-195.049503 a.u.
G(total):	-195.082336 a.u.

Phenylsilane (PhSiH₃)



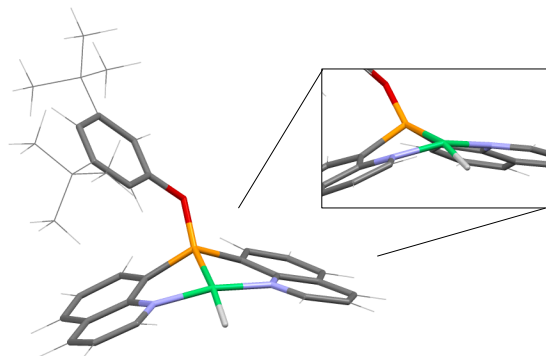
$E_{\text{elec}}^{\text{BS1}}$:	-522.2900405 a.u.
$E_{\text{elec}}^{\text{SMD,BS2}}$:	-522.6440873 a.u.
E_{disp} :	-0.013560056 a.u.
H correc:	0.123913 a.u.
G correc:	0.083211 a.u.
H(total):	-522.520174 a.u.
G(total):	-522.560876 a.u.

PhSiH₂Cl



$E_{\text{elec}}^{\text{BS1}}$:	-981.6574432 a.u.
$E_{\text{elec}}^{\text{SMD,BS2}}$:	-982.1734599 a.u.
E_{disp} :	-0.015585648 a.u.
H correc:	0.119151 a.u.
G correc:	0.074978 a.u.
H(total):	-982.054309 a.u.
G(total):	-982.098482 a.u.

(NPN)Ni-H⁺

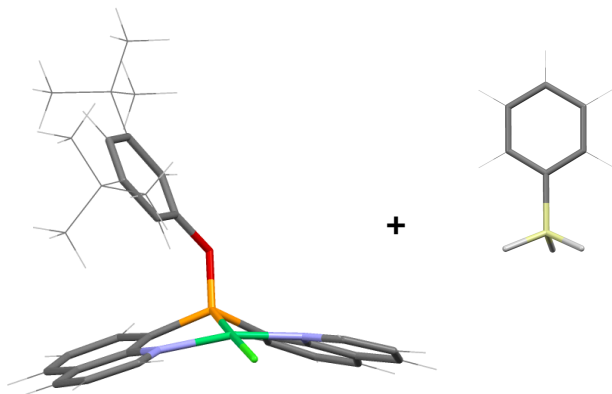


$E_{\text{elec}}^{\text{BS1}}$:	-1933.9153105 a.u.
$E_{\text{elec}}^{\text{SMD,BS2}}$:	-1935.626074 a.u.
E_{disp} :	-0.103849793 a.u.
H correc:	0.62173 a.u.
G correc:	0.525153 a.u.
H(total):	-1935.004344 a.u.
G(total):	-1935.100921 a.u.

The sum of the energies of two “Cyclopentene”, two “PhSiH₃”, one “PhSiH₂Cl” and “(NPN)Ni-H⁺” serves as the reference of energies for the computational study.

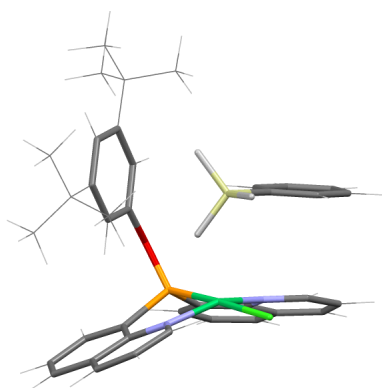
Formation of the Ni-H catalyst

(NPN)Ni-Cl⁺ (Monomer precatalyst with the chloride atom) + PhSiH₃



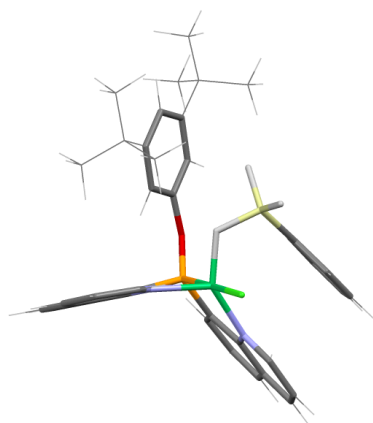
(NPN)Ni-Cl	
E _{elec} ^{BS1} :	-2393.2995747 a.u.
E _{elec} ^{SMD,BS2} :	-2395.172168 a.u.
E _{disp} :	-0.108388279 a.u.
H correc:	0.617117 a.u.
G correc:	0.516115 a.u.
H(total):	-2394.555051 a.u.
G(total):	-2394.656053 a.u.
PhSiH3	
< Data in "Reference" section. >	
Sum of both structures	
H(total):	-2917.075225 a.u.
G(total):	-2917.216929 a.u.
ΔH°:	-10.40 kcal/mol
ΔG°:	-11.00 kcal/mol

Cl - (NPN)Ni-Cl⁺ catalyst and the phenylsilane interacting



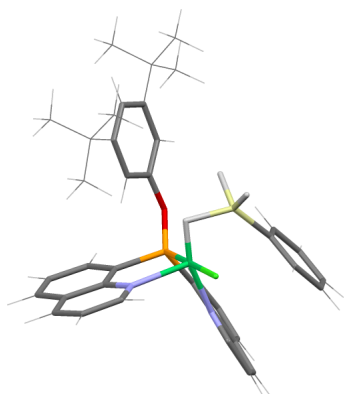
E _{elec} ^{BS1} :	-2915.6173597 a.u.
E _{elec} ^{SMD,BS2} :	-2917.829811 a.u.
E _{disp} :	-0.146666631 a.u.
H correc:	0.744107 a.u.
G correc:	0.621131 a.u.
H(total):	-2917.085704 a.u.
G(total):	-2917.20868 a.u.
ΔH°:	-16.97 kcal/mol
ΔG°:	-5.82 kcal/mol

TS_{Si} – TS for the coordination of phenylsilane to the Ni-Cl catalyst



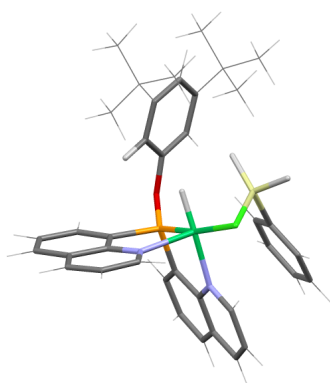
E _{elec} ^{BS1} :	-2915.6102940 a.u.
E _{elec} ^{SMD,BS2} :	-2917.817541 a.u.
E _{disp} :	-0.148419117 a.u.
H correc:	0.742882 a.u.
G correc:	0.622167 a.u.
H(total):	-2917.074659 a.u.
G(total):	-2917.195374 a.u.
ΔH°:	-10.04 kcal/mol
ΔG°:	2.53 kcal/mol

Si_2 - Precatalytic structure. Phenylsilane already coordinated to the Ni-Cl catalyst



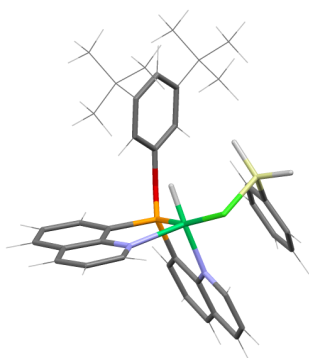
E_{elec}^{BS1} :	-2915.6140863 a.u.
$E_{elec}^{SMD,BS2}$:	-2917.822068 a.u.
E_{disp} :	-0.145878903 a.u.
H correc:	0.744162 a.u.
G correc:	0.622712 a.u.
H(total):	-2917.077906 a.u.
G(total):	-2917.199356 a.u.
ΔH° :	-12.08 kcal/mol
ΔG° :	0.03 kcal/mol

TS_Cl_H - TS of the formation of the $[(NPN)Ni-H]^+$ catalyst and SiH_2PhCl



E_{elec}^{BS1} :	-2915.6001614 a.u.
$E_{elec}^{SMD,BS2}$:	-2917.807301 a.u.
E_{disp} :	-0.146746882 a.u.
H correc:	0.742698 a.u.
G correc:	0.621891 a.u.
H(total):	-2917.064603 a.u.
G(total):	-2917.18541 a.u.
ΔH° :	-3.73 kcal/mol
ΔG° :	8.78 kcal/mol

H - $(NPN)Ni-H^+$ catalyst already formed with the SiH_2PhCl silane still interacting with the Ni atom.



E_{elec}^{BS1} :	-2915.6084746 a.u.
$E_{elec}^{SMD,BS2}$:	-2917.815689 a.u.
E_{disp} :	-0.143153112 a.u.
H correc:	0.743322 a.u.
G correc:	0.618645 a.u.
H(total):	-2917.072367 a.u.
G(total):	-2917.197044 a.u.
ΔH° :	-8.61 kcal/mol
ΔG° :	1.48 kcal/mol

H (S=1)
Optimized structure.

E_{elec}^{BS1} :	-2915.6146681 a.u.
$E_{elec}^{SMD,BS2}$:	-2917.820155 a.u.
E_{disp} :	-0.144540025 a.u.
H correc:	0.742535 a.u.
G correc:	0.621996 a.u.
H(total):	-2917.07762 a.u.
G(total):	-2917.198159 a.u.
ΔH° :	-11.9 kcal/mol
ΔG° :	0.78 kcal/mol

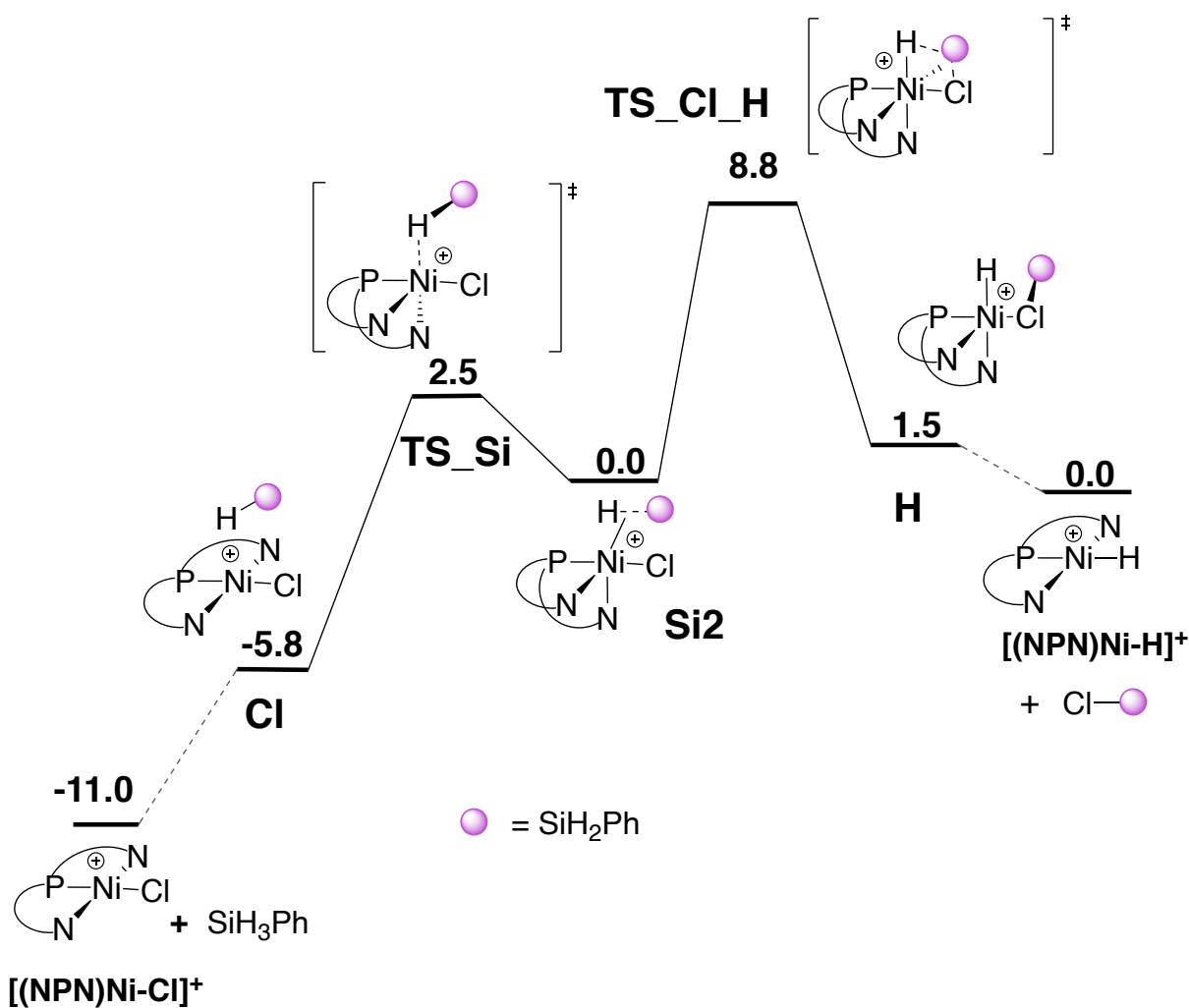
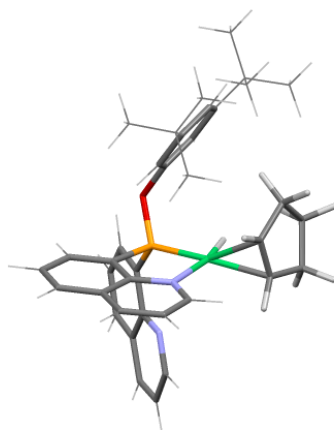


Figure S4: Gibbs energy profile (kcal/mol) for the reaction of $[(\text{NPN})\text{Ni-Cl}]^+$ and SiH_3Ph to form $[(\text{NPN})\text{Ni-H}]^+$ and ClSiH_2Ph . PBE0-D3/BS2-SMD(o-dichlorobenzene) level of theory (G° -dichlorobenzene, PBE0-D3BJ, BS2), singlet electronic state.

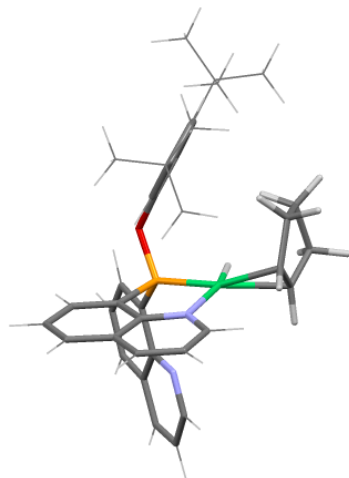
Cycle with the $[(\text{NPN})\text{Ni-H}]^+$ catalyst

I - Coordination of the cyclopentene



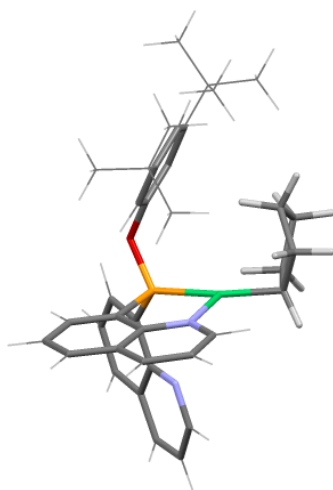
$E_{\text{elec}}^{\text{BS1}}$	-2128.9119682 a.u.
$E_{\text{elec}}^{\text{SMD,BS2}}$	-2130.826042 a.u.
E_{disp}	-0.127565018 a.u.
H correc:	0.747255 a.u.
G correc:	0.631831 a.u.
H(total):	-2130.078787 a.u.
G(total):	-2130.194211 a.u.
ΔH°	-15.65 kcal/mol
ΔG°	-6.87 kcal/mol

TS_I_II - TS for the C-H bond formation



$E_{\text{elec}}^{\text{BS1}}$:	-2128.9084467 a.u.
$E_{\text{elec}}^{\text{SMD,BS2}}$:	-2130.821855 a.u.
E_{disp} :	-0.128309284 a.u.
H correc:	0.746431 a.u.
G correc:	0.634937 a.u.
H(total):	-2130.075424 a.u.
G(total):	-2130.186918 a.u.
ΔH° :	-13.54 kcal/mol
ΔG° :	-2.3 kcal/mol

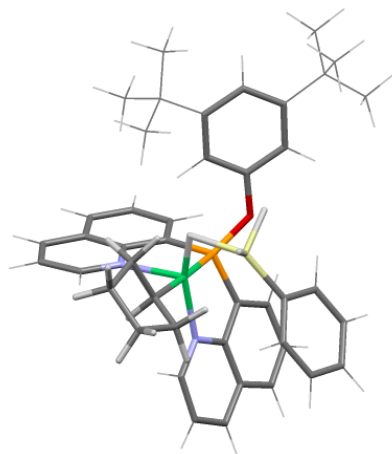
II - Ni-Alkyl post TS. Agostic interaction.



$E_{\text{elec}}^{\text{BS1}}$:	-2128.9321957 a.u.
$E_{\text{elec}}^{\text{SMD,BS2}}$:	-2130.842773 a.u.
E_{disp} :	-0.129075942 a.u.
H correc:	0.749682 a.u.
G correc:	0.637437 a.u.
H(total):	-2130.093091 a.u.
G(total):	-2130.205336 a.u.
ΔH° :	-24.63 kcal/mol
ΔG° :	-13.85 kcal/mol

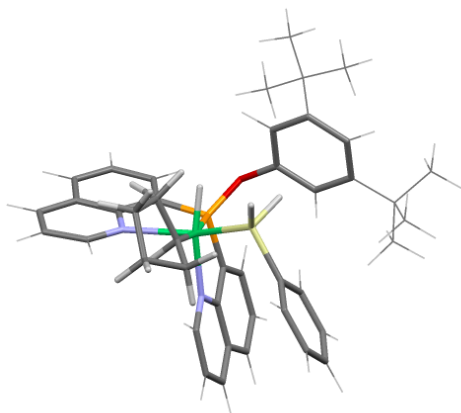
Formation of the C-Si bond = Silane Product

III - Inclusion of the silane forming the Ni-C-Si-H ordering



$E_{\text{elec}}^{\text{BS1}}$:	-2651.2378692 a.u.
$E_{\text{elec}}^{\text{SMD,BS2}}$:	-2653.494659 a.u.
E_{disp} :	-0.164633289 a.u.
H correc:	0.877949 a.u.
G correc:	0.748202 a.u.
H(total):	-2652.61671 a.u.
G(total):	-2652.746457 a.u.
ΔH° :	-26.79 kcal/mol
ΔG° :	-1.46 kcal/mol

TSA1 - TS for the C-Si bond formation

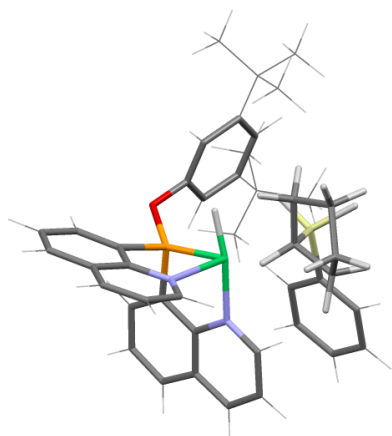


$E_{\text{elec}}^{\text{BS1}}$:	-2651.2259829 a.u.
$E_{\text{elec}}^{\text{SMD,BS2}}$:	-2653.484661 a.u.
E_{disp} :	-0.164558276 a.u.
H correc:	0.876423 a.u.
G correc:	0.747919 a.u.
H(total):	-2652.608238 a.u.
G(total):	-2652.736742 a.u.
ΔH° :	-21.47 kcal/mol
ΔG° :	4.64 kcal/mol

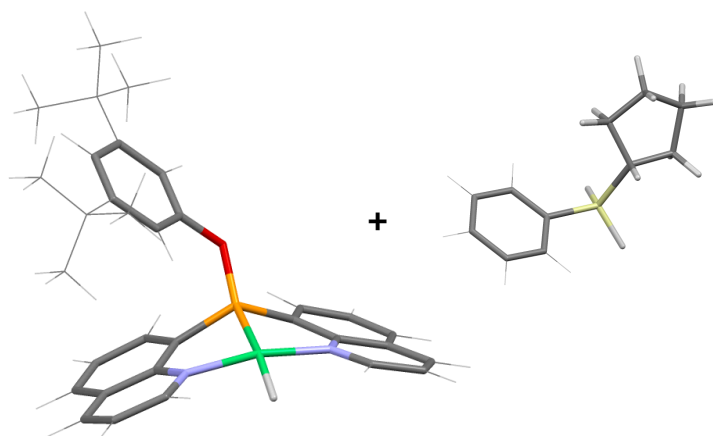
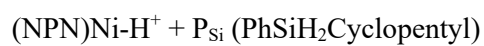
TSA1 (S=1)
Optimized structure.

$E_{\text{elec}}^{\text{BS1}}$:	-2651.2004204 a.u.
$E_{\text{elec}}^{\text{SMD,BS2}}$:	-2653.46473 a.u.
E_{disp} :	-0.162812517 a.u.
H correc:	0.874676 a.u.
G correc:	0.745141 a.u.
H(total):	-2652.590054 a.u.
G(total):	-2652.719589 a.u.
ΔH° :	-10.06 kcal/mol
ΔG° :	15.4 kcal/mol

IV - Product post TS. New silane formed: $\text{PhSiH}_2\text{Cyclopentyl}$, with still a strong interaction with the Ni atom.



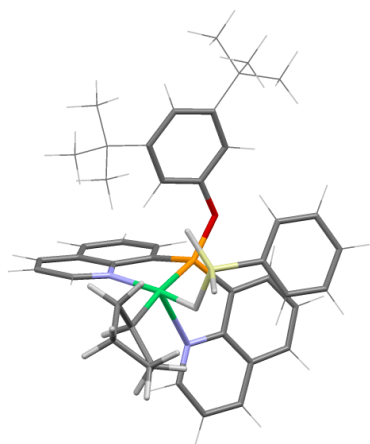
$E_{\text{elec}}^{\text{BS1}}$:	-2651.2402656 a.u.
$E_{\text{elec}}^{\text{SMD,BS2}}$:	-2653.499737 a.u.
E_{disp} :	-0.162537437 a.u.
H correc:	0.877039 a.u.
G correc:	0.745571 a.u.
H(total):	-2652.622698 a.u.
G(total):	-2652.754166 a.u.
ΔH° :	-30.55 kcal/mol
ΔG° :	-6.3 kcal/mol



(NPN)Ni-H	
$E_{\text{elec}}^{\text{BS1}}$:	-1933.9153105 a.u.
$E_{\text{elec}}^{\text{SMD,BS2}}$:	-1935.626074 a.u.
E_{disp} :	-0.103849793 a.u.
H correc:	0.62173 a.u.
G correc:	0.525153 a.u.
H(total):	-1935.004344 a.u.
G(total):	-1935.100921 a.u.
PhSiH ₂ Cyclopentyl	
$E_{\text{elec}}^{\text{BS1}}$:	-717.3006955 a.u.
$E_{\text{elec}}^{\text{SMD,BS2}}$:	-717.8647434 a.u.
E_{disp} :	-0.028257489 a.u.
H correc:	0.252766 a.u.
G correc:	0.197236 a.u.
H(total):	-717.611977 a.u.
G(total):	-717.667507 a.u.
Sum of both structures	
H(total):	-2652.616321 a.u.
G(total):	-2652.768428 a.u.
ΔH° :	-26.54 kcal/mol
ΔG° :	-15.25 kcal/mol

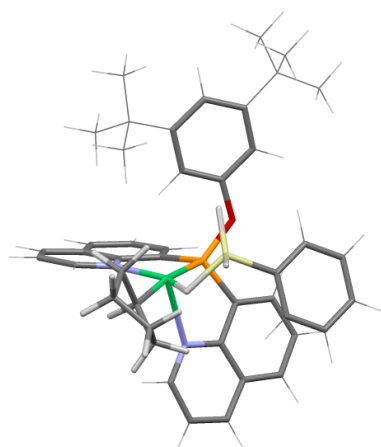
Formation of the second C-C bond = Alkane Product

V - Insertion of the silane (PhSiH₃) forming the Ni-C-H-Si sequence.



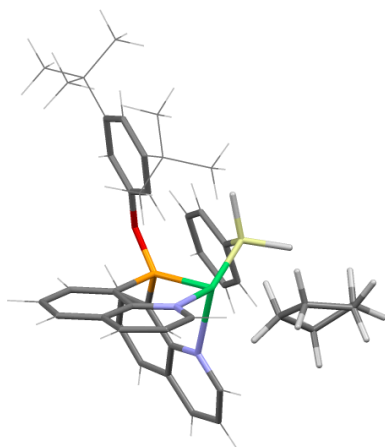
$E_{\text{elec}}^{\text{BS1}}$:	-2651.2347572 a.u.
$E_{\text{elec}}^{\text{SMD,BS2}}$:	-2653.490243 a.u.
E_{disp} :	-0.163598294 a.u.
H correc:	0.878067 a.u.
G correc:	0.745374 a.u.
H(total):	-2652.612176 a.u.
G(total):	-2652.744869 a.u.
ΔH° :	-23.94 kcal/mol
ΔG° :	-0.46 kcal/mol

TSA2 - TS to form the second C-H bond = Alkane generation

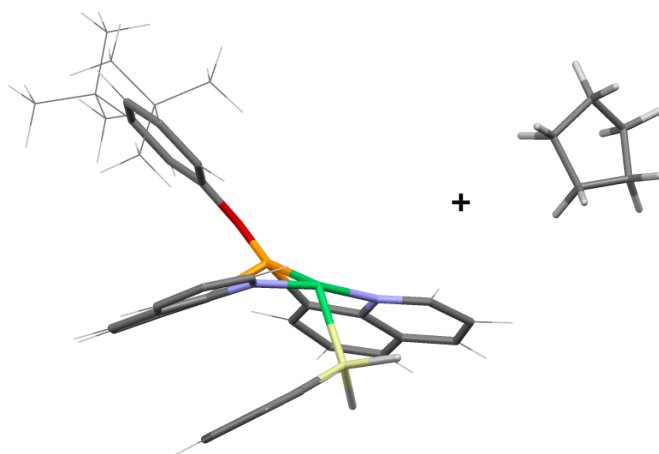
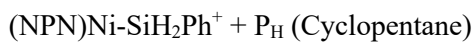


$E_{\text{elec}}^{\text{BS1}}$:	-2651.2304584 a.u.
$E_{\text{elec}}^{\text{SMD,BS2}}$:	-2653.48626 a.u.
E_{disp} :	-0.16433723 a.u.
H correc:	0.875948 a.u.
G correc:	0.74556 a.u.
H(total):	-2652.610312 a.u.
G(total):	-2652.7407 a.u.
ΔH° :	-22.77 kcal/mol
ΔG° :	2.15 kcal/mol

VI - Direct product post the alkane generation, where the alkane group is still interacting with Ni and the catalyst already has the (NPN)Ni-Silyl form.



$E_{\text{elec}}^{\text{BS1}}$:	-2651.2587353 a.u.
$E_{\text{elec}}^{\text{SMD,BS2}}$:	-2653.518282 a.u.
E_{disp} :	-0.163091377 a.u.
H correc:	0.881858 a.u.
G correc:	0.748703 a.u.
H(total):	-2652.636424 a.u.
G(total):	-2652.769579 a.u.
ΔH° :	-39.16 kcal/mol
ΔG° :	-15.97 kcal/mol



(NPN)Ni-SiH ₂ Ph	
E _{elec} ^{BS1} :	-2455.0582735 a.u.
E _{elec} ^{SMD,BS2} :	-2457.110407 a.u.
E _{disp} :	-0.134034048 a.u.
H correc:	0.730567 a.u.
G correc:	0.617004 a.u.
H(total):	-2456.37984 a.u.
G(total):	-2456.493403 a.u.
Cyclopentane	
E _{elec} ^{BS1} :	-196.18421 a.u.
E _{elec} ^{SMD,BS2} :	-196.3986418 a.u.
E _{disp} :	-0.009789817 a.u.
H correc:	0.147083 a.u.
G correc:	0.109816 a.u.
H(total):	-196.251559 a.u.
G(total):	-196.288826 a.u.
Sum of both structures	
H(total):	-2652.631399 a.u.
G(total):	-2652.782229 a.u.
ΔH°:	-36.01 kcal/mol
ΔG°:	-23.91 kcal/mol

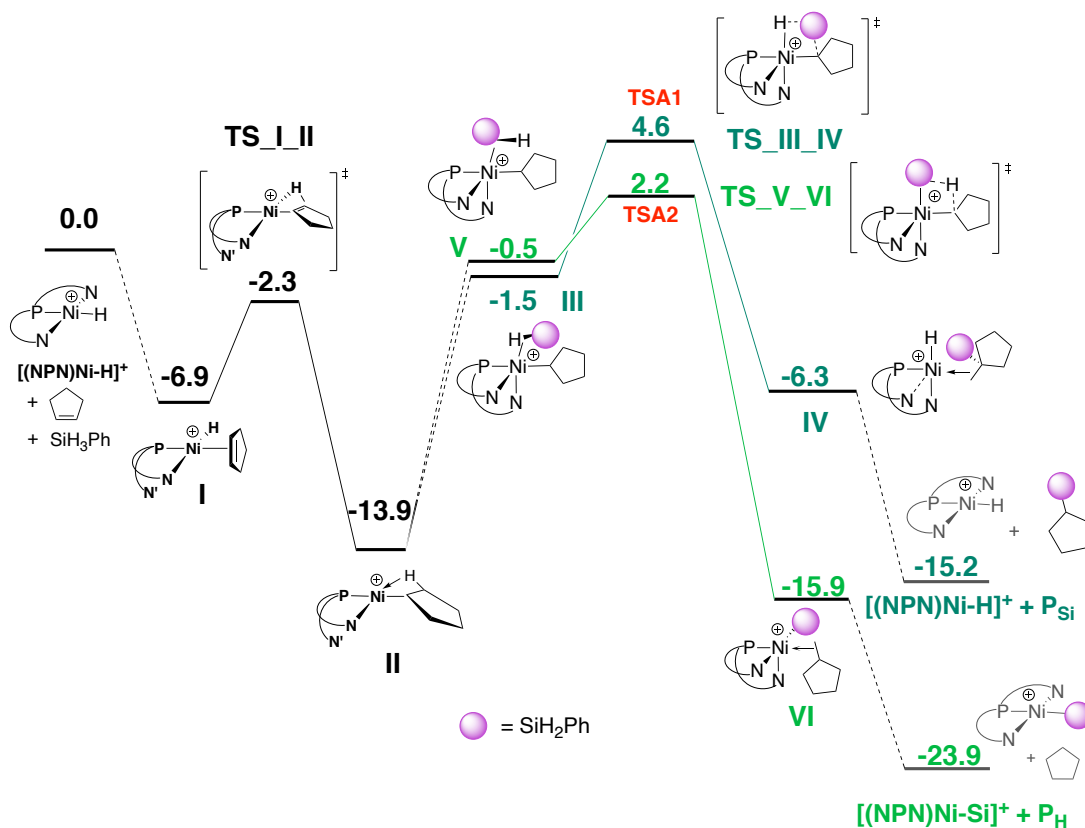
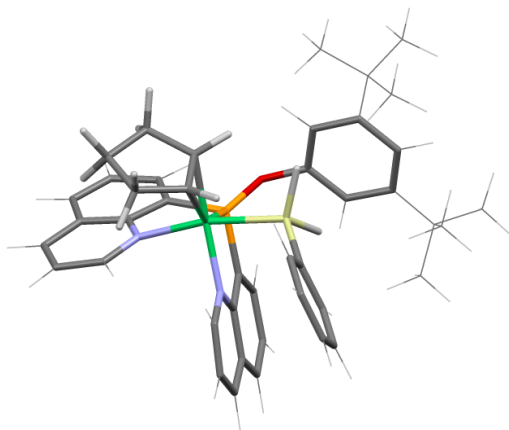


Figure S5: Gibbs energy profile (kcal/mol) for the catalytic hydrosilation of cyclopentene by SiH₃Ph assisted by [(NPN)Ni-H]⁺. The pathways for the formation of cyclopentane and PhSiH₂-C₅H₉ are shown. PBE0-D3/BS2-SMD(o-dichlorobenzene), PBE0-D3BJ, BS2², singlet electronic state.

Cycle with the [(NPN)Ni-Silyl]⁺ catalyst

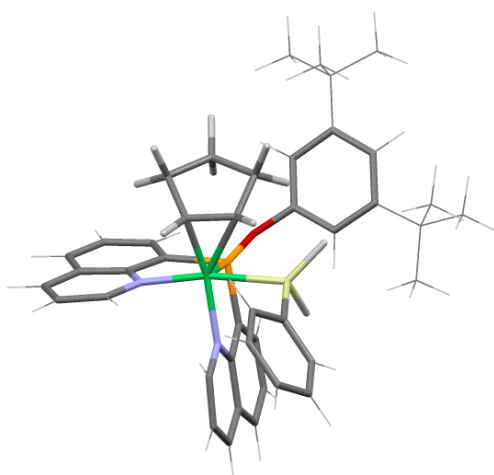
Formation of the Calkene-Si bond

VII - Entrance of the cyclopentene



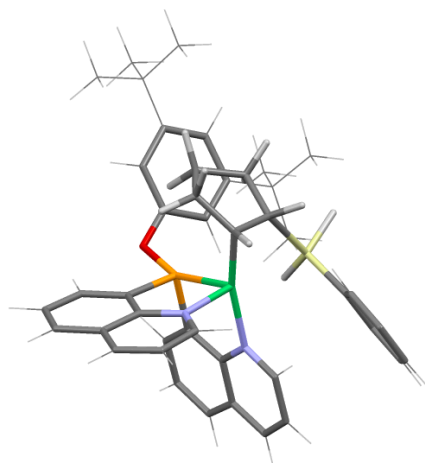
E _{elec} ^{BS1} :	-2650.0562238 a.u.
E _{elec} ^{SMD,BS2} :	-2652.309262 a.u.
E _{disp} :	-0.161736876 a.u.
H correc:	0.855745 a.u.
G correc:	0.730564 a.u.
H(total):	-2651.453517 a.u.
G(total):	-2651.578698 a.u.
ΔH ^o :	-51.17 kcal/mol
ΔG ^o :	-25.76 kcal/mol

TS_VII_VIII - TS for the initial C-Si bond formation



E _{elec} ^{BS1} :	-2650.0490611 a.u.
E _{elec} ^{SMD,BS2} :	-2652.300654 a.u.
E _{disp} :	-0.161685444 a.u.
H correc:	0.856289 a.u.
G correc:	0.732 a.u.
H(total):	-2651.444365 a.u.
G(total):	-2651.568654 a.u.
ΔH ^o :	-45.43 kcal/mol
ΔG ^o :	-19.46 kcal/mol

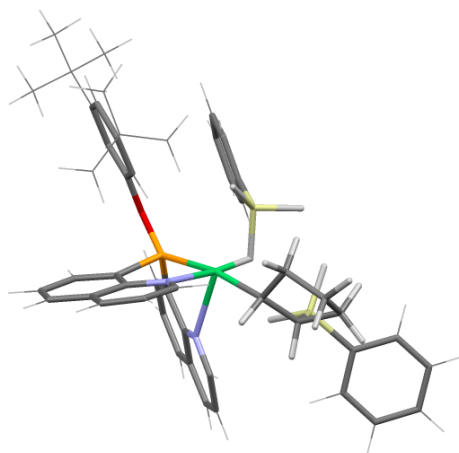
VIII - Silylalkyl already formed with an interaction between Ni and the C-Si bond.



E _{elec} ^{BS1} :	-2650.0511189 a.u.
E _{elec} ^{SMD,BS2} :	-2652.300985 a.u.
E _{disp} :	-0.160896093 a.u.
H correc:	0.856709 a.u.
G correc:	0.729047 a.u.
H(total):	-2651.444276 a.u.
G(total):	-2651.571938 a.u.
ΔH ^o :	-45.38 kcal/mol
ΔG ^o :	-21.52 kcal/mol

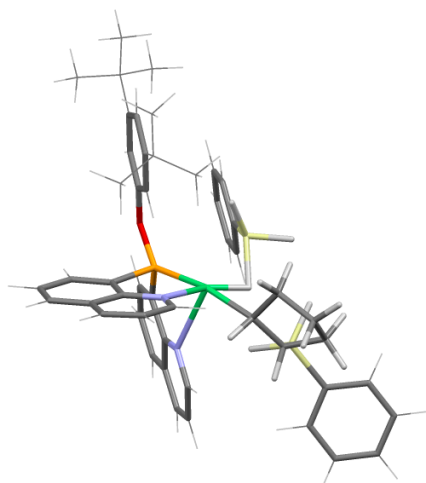
Formation of the C-H bond = Silane product

IX - Entrance of the second silane forming the Ni-C-H-Si interaction



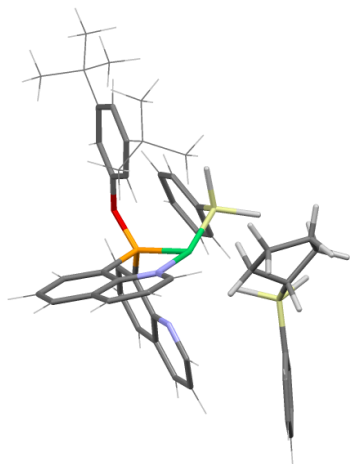
$E_{\text{elec}}^{\text{BS1}}$:	-3172.3569546 a.u.
$E_{\text{elec}}^{\text{SMD,BS2}}$:	-3174.960052 a.u.
E_{disp} :	-0.191173205 a.u.
H correc:	0.983618 a.u.
G correc:	0.836591 a.u.
H(total):	-3173.976434 a.u.
G(total):	-3174.123461 a.u.
ΔH° :	-52.9 kcal/mol
ΔG° :	-15.65 kcal/mol

TSB2 - TS of the formation of the C-H bond for the Ni-Si catalyst = Formation of the PhSiH₂Cyclopentyl product

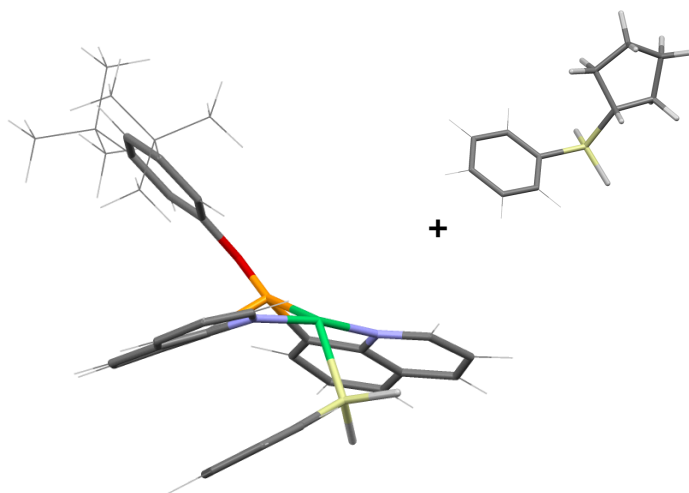
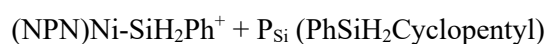


$E_{\text{elec}}^{\text{BS1}}$:	-3172.3489175 a.u.
$E_{\text{elec}}^{\text{SMD,BS2}}$:	-3174.952556 a.u.
E_{disp} :	-0.190149249 a.u.
H correc:	0.981946 a.u.
G correc:	0.835433 a.u.
H(total):	-3173.97061 a.u.
G(total):	-3174.117123 a.u.
ΔH° :	-49.24 kcal/mol
ΔG° :	-11.67 kcal/mol

X - Direct product post the formation of the PhSiH₂Cyclopentyl silane by the Ni-Silyl catalyst.
Adduct between the catalyst and substrate still formed.



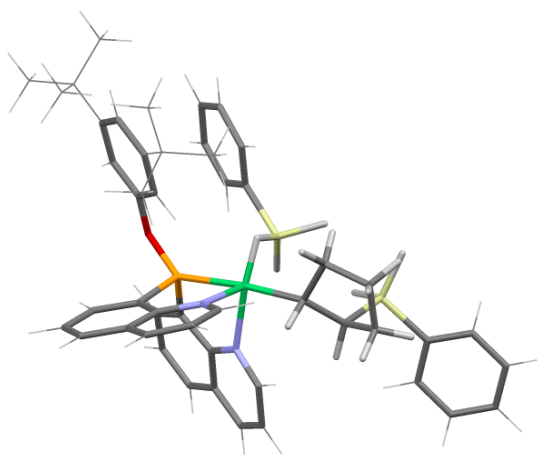
$E_{\text{elec}}^{\text{BS1}}$:	-3172.3798529 a.u.
$E_{\text{elec}}^{\text{SMD,BS2}}$:	-3174.984164 a.u.
E_{disp} :	-0.1932341 a.u.
H correc:	0.986646 a.u.
G correc:	0.838412 a.u.
H(total):	-3173.997518 a.u.
G(total):	-3174.145752 a.u.
ΔH° :	-66.13 kcal/mol
ΔG° :	-29.64 kcal/mol



(NPN)Ni-SiH ₂ Ph	
E _{elec} ^{BS1} :	-2455.0582735 a.u.
E _{elec} ^{SMD,BS2} :	-2457.110407 a.u.
E _{disp} :	-0.134034048 a.u.
H correc:	0.730567 a.u.
G correc:	0.617004 a.u.
H(total):	-2456.37984 a.u.
G(total):	-2456.493403 a.u.
PhSiH ₂ Cyclopentyl	
E _{elec} ^{BS1} :	-717.3006955 a.u.
E _{elec} ^{SMD,BS2} :	-717.8647434 a.u.
E _{disp} :	-0.028257489 a.u.
H correc:	0.252766 a.u.
G correc:	0.197236 a.u.
H(total):	-717.611977 a.u.
G(total):	-717.667507 a.u.
Sum of both structures	
H(total):	-3370.243376 a.u.
G(total):	-3370.449736 a.u.
ΔH ^o :	-62.55 kcal/mol
ΔG ^o :	-39.15 kcal/mol

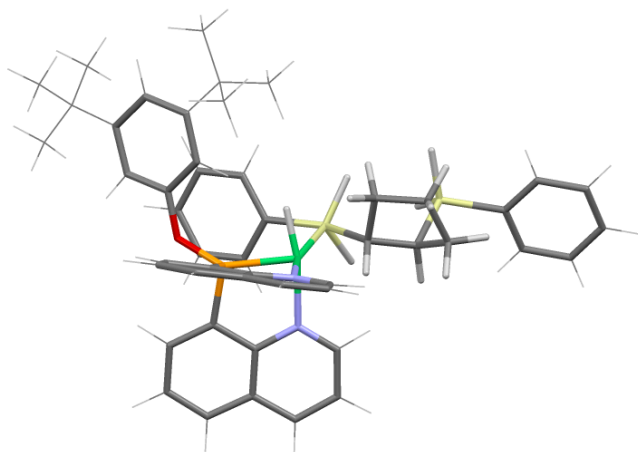
Formation of the second C-Si bond = Double-silylated products

XI - Entrance of the second silane forming the Ni-C-Si-H interaction



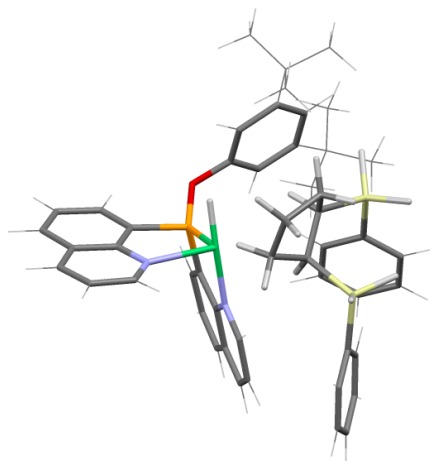
E _{elec} ^{BS1} :	-3172.3464943 a.u.
E _{elec} ^{SMD,BS2} :	-3174.95252 a.u.
E _{disp} :	-0.188986475 a.u.
H correc:	0.983189 a.u.
G correc:	0.836876 a.u.
H(total):	-3173.969331 a.u.
G(total):	-3174.115644 a.u.
ΔH ^o :	-48.44 kcal/mol
ΔG ^o :	-10.75 kcal/mol

TSB1 - TS of the formation of the second C-Si bond by the Ni-Si catalyst = Double-silylated products.



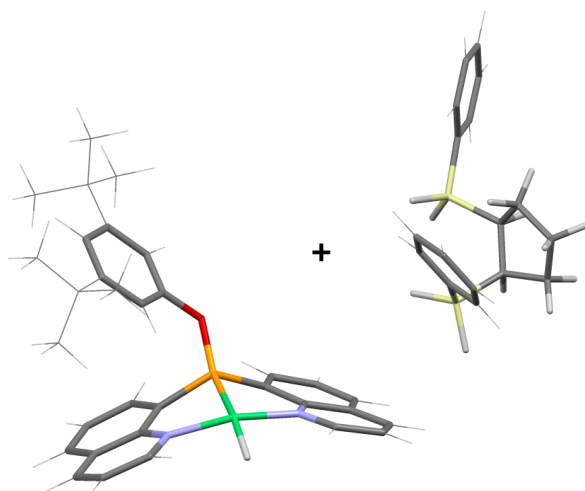
$E_{\text{elec}}^{\text{BS1}}$:	-3172.3420472 a.u.
$E_{\text{elec}}^{\text{SMD,BS2}}$:	-3174.950522 a.u.
E_{disp} :	-0.186400048 a.u.
H correc:	0.982492 a.u.
G correc:	0.836559 a.u.
H(total):	-3173.96803 a.u.
G(total):	-3174.113963 a.u.
ΔH° :	-47.62 kcal/mol
ΔG° :	-9.69 kcal/mol

XII - Direct products of the double-silylation. Adducts between the catalyst and the double silane still formed.



$E_{\text{elec}}^{\text{BS1}}$:	-3172.3642086 a.u.
$E_{\text{elec}}^{\text{SMD,BS2}}$:	-3174.967479 a.u.
E_{disp} :	-0.193831415 a.u.
H correc:	0.984004 a.u.
G correc:	0.839558 a.u.
H(total):	-3173.983475 a.u.
G(total):	-3174.127921 a.u.
ΔH° :	-57.31 kcal/mol
ΔG° :	-18.45 kcal/mol

$(\text{NPN})\text{Ni-H}^+ + \text{P}_{\text{Si2}} (\text{PhSiH}_2\text{AlkSiH}_2\text{Ph})$



(NPN)Ni-H	
$E_{\text{elec}}^{\text{BS1}}$:	-1933.9153105 a.u.
$E_{\text{elec}}^{\text{SMD,BS2}}$:	-1935.626074 a.u.
E_{disp} :	-0.103849793 a.u.
H correc:	0.62173 a.u.
G correc:	0.525153 a.u.
H(total):	-1935.004344 a.u.
G(total):	-1935.100921 a.u.
PhSiH ₂ AlkSiH ₂ Ph	
$E_{\text{elec}}^{\text{BS1}}$:	-1238.4177454 a.u.
$E_{\text{elec}}^{\text{SMD,BS2}}$:	-1239.329123 a.u.
E_{disp} :	-0.051710616 a.u.
H correc:	0.358578 a.u.
G correc:	0.287023 a.u.
H(total):	-1238.970545 a.u.
G(total):	-1239.0421 a.u.
Sum of both structures	
H(total):	-3370.226448 a.u.
G(total):	-3370.431847 a.u.
ΔH° :	-51.93 kcal/mol
ΔG° :	-27.93 kcal/mol

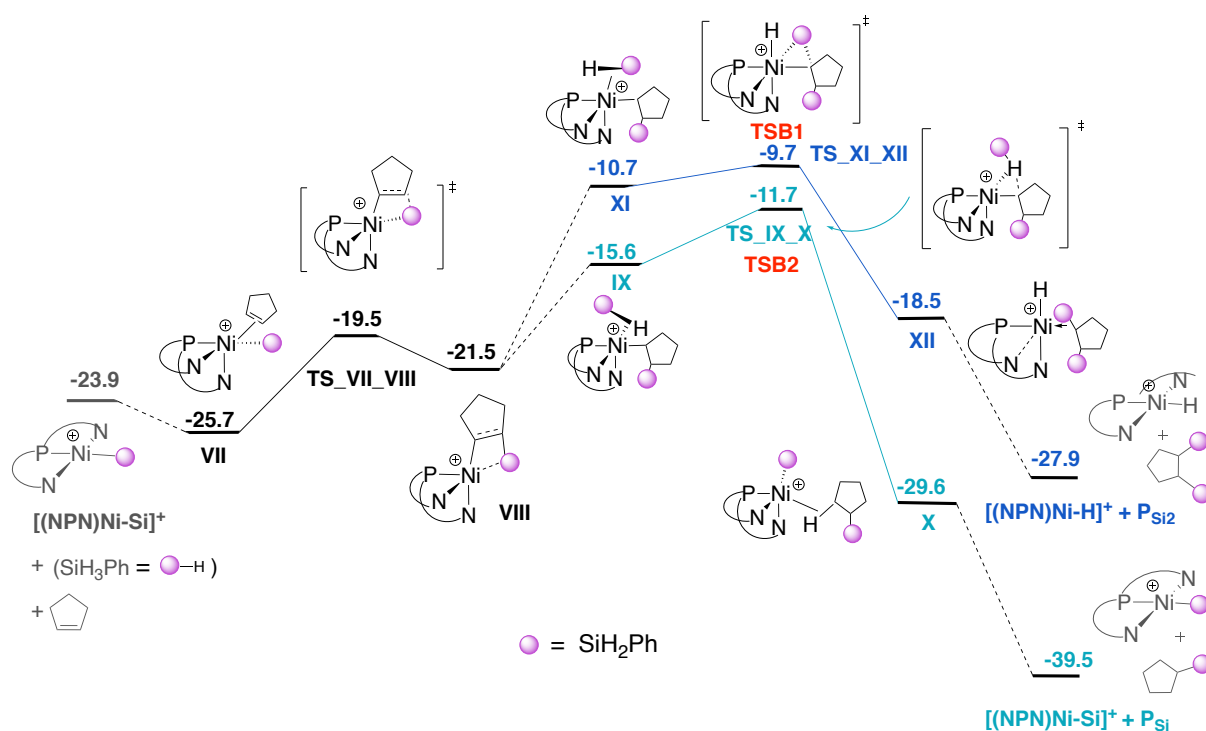
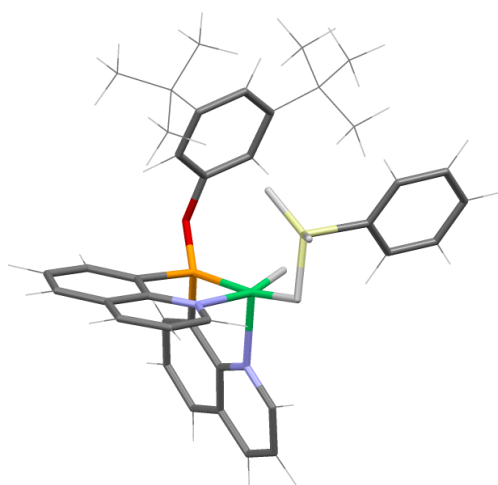


Figure S6: Gibbs energy profile (kcal/mol) for the catalytic cycle for the hydrosilylation of cyclopentene by SiH_3Ph assisted $[(\text{NPN})\text{Ni}-\text{SiH}_2\text{Ph}]^+$. The reaction pathways for the formation of $\text{C}_5\text{H}_9(\text{SiH}_2\text{Ph})$ and $1,2(\text{SiH}_2\text{Ph})\text{C}_5\text{H}_8$ are shown. PBE0-D3/BS2-SMD(o-dichlorobenzene) level of theory (G^o-dichlorobenzene, PBE0-D3BJ, BS2), singlet electronic state.

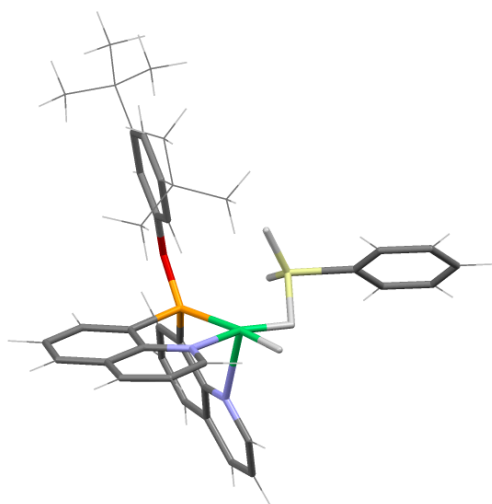
$[(\text{NPN})\text{Ni}-\text{H}]^+ \longleftrightarrow [(\text{NPN})\text{Ni}-\text{Silyl}]^+$ interconversion mediated by a silane moiety

$(\text{NPN})\text{Ni}-\text{H}^+_{\text{PhSiH}_3}$ - Ni-H catalyst interacting with the SiH_3Ph silane



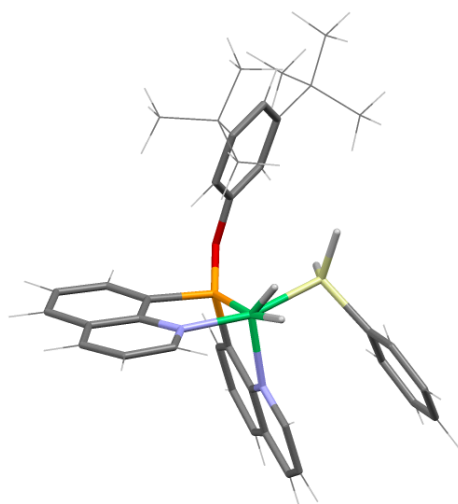
$E_{\text{elec}}^{\text{BS1}}$:	-2456.2395857 a.u.
$E_{\text{elec}}^{\text{SMD,BS2}}$:	-2458.296786 a.u.
E_{disp} :	-0.135530731 a.u.
H correc:	0.748512 a.u.
G correc:	0.629011 a.u.
H(total):	-2457.548274 a.u.
G(total):	-2457.667775 a.u.
ΔH° :	-14.91 kcal/mol
ΔG° :	-3.75 kcal/mol

TS_H_PhSiH₂ - TS of the reaction of the silane with the Ni-H catalyst to form the Ni-Silyl catalyst



$E_{\text{elec}}^{\text{BS1}}$:	-2456.2225893 a.u.
$E_{\text{elec}}^{\text{SMD,BS2}}$:	-2458.278283 a.u.
E_{disp} :	-0.130807885 a.u.
H correc:	0.746237 a.u.
G correc:	0.627427 a.u.
H(total):	-2457.532046 a.u.
G(total):	-2457.650856 a.u.
ΔH° :	-4.72 kcal/mol
ΔG° :	6.87 kcal/mol

(NPN)Ni-SiH₂Ph⁺_H₂ - Ni-Silyl catalyst already formed by a silane moiety. The H₂ molecule which has been originated is still interacting with the catalyst



$E_{\text{elec}}^{\text{BS1}}$:	-2456.2411557 a.u.
$E_{\text{elec}}^{\text{SMD,BS2}}$:	-2458.297136 a.u.
E_{disp} :	-0.137558056 a.u.
H correc:	0.748628 a.u.
G correc:	0.626149 a.u.
H(total):	-2457.548508 a.u.
G(total):	-2457.670987 a.u.
ΔH° :	-15.05 kcal/mol
ΔG° :	-5.77 kcal/mol

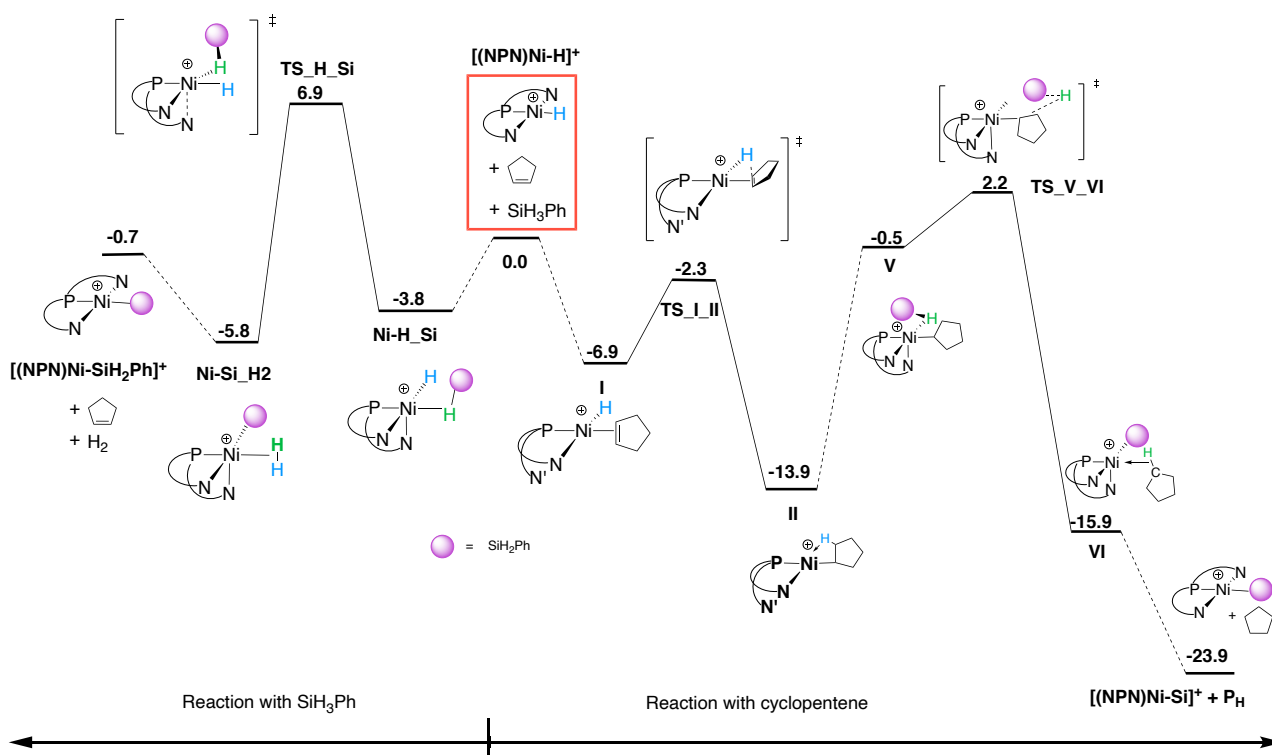


Figure S7: Gibbs Energy profile (kcal/mol) for the reaction of $[(\text{NPN})\text{Ni-H}]^+$ with silane (left-hand side) and with cyclopentene (right-hand side). PBE0-D3/BS2-SMD(o-dichlorobenzene) level of theory ($G^{\text{o-dichlorobenzene, PBE0-D3BJ, BS2}}$), singlet electronic state.

Structural variety and multiple pathways

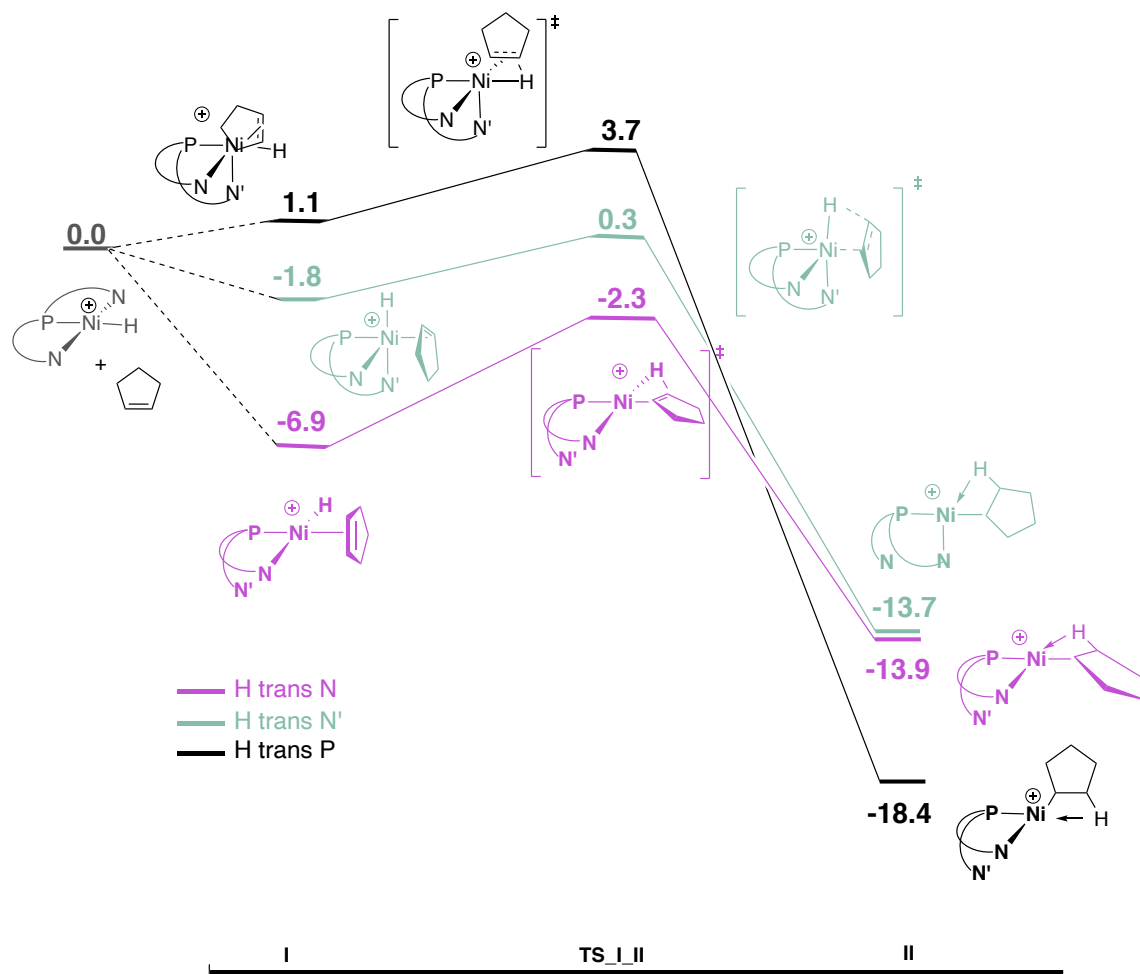
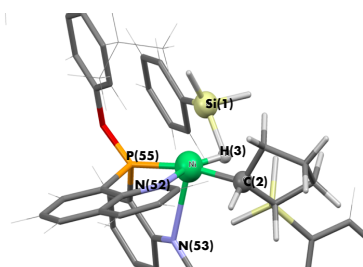


Figure S8: Gibbs energy profiles of the several pathways associated with the insertion of the cyclopentene in the Ni-H bond of $[(\text{NPN})\text{NiH}]^+$. PBE0-D3/BS2-SMD(o-dichlorobenzene) level of theory ($G^{\text{o-dichlorobenzene, PBE0-D3BJ, BS2}}$), singlet electronic state.

(4) NBO analysis of TSB2

NBO Charges	
Ni	0.44534
C	-0.60762
H	-0.03494
Si	0.96448



===== COMPOUND: TSB2 =====

=== NBO numbering ===

LP

Ni: 72(1.98e-),73(1.97e-),74(1.97e-),53(1.90e-)

N₅₂: 78(1.81e-)

N₅₃: 79(1.86e-)

P₅₅: 82(1.60e-)

BD

C(2)-Ni: 86(1.90e-)

3Center: Si(1)-H(3)-Ni: 216(1.66e-) / 37.19% of Si(1), 53.87% of H(3), 8.94% of Ni

BD*

C(2)-Ni: 222(0.65e-)

3Cn: Si(1)-H(3)-Ni: 352(0.22-) / 31.57% of Si(1), 44.42% of H(3), 24.00% of Ni

3C*: Si(1)-H(3)-Ni: 353(0.14e-) / 31.24% of Si(1), 1.71% of H(3), 67.05% of Ni

=== SECOND ORDER PERTURBATION THEORY ANALYSIS ===

from	72. LP(1) Ni	to	352. 3Cn Si(1)-H(3)-Ni	3.39 kcal/mol
from	72. LP(1) Ni	to	353. 3C* Si(1)-H(3)-Ni	8.61 kcal/mol
from	75. LP(4) Ni	to	352. 3Cn Si(1)-H(3)-Ni	3.62 kcal/mol
from	75. LP(4) Ni	to	353. 3C* Si(1)-H(3)-Ni	8.30 kcal/mol
from	78. LP N ₅₂	to	352. 3Cn Si(1)-H(3)-Ni	14.03 kcal/mol
from	78. LP N ₅₂	to	353. 3C* Si(1)-H(3)-Ni	21.37 kcal/mol
from	82. LP P ₅₅	to	222. BD* C(2)-Ni	66.39 kcal/mol
from	82. LP P ₅₅	to	352. 3Cn Si(1)-H(3)-Ni	56.59 kcal/mol
from	82. LP P ₅₅	to	353. 3C* Si(1)-H(3)-Ni	54.68 kcal/mol
from	216. 3C Si(1)-H-Ni	to	222. BD* C(2)-Ni	129.51 kcal/mol

=== NATURAL LOCALIZED MOLECULAR ORBITALS (NLMO) ANALYSIS ===

Orbital 72. (2.00e-): 98.83% LP(1) Ni; 0.05% on Si(1); 0.02% on H(3); 0.06% on C(2).

Orbital 75. (2.00e-): 94.99% LP(4) Ni; 1.77% on Si(1); 1.52% on H(3); 0.37% on C(2).

Orbital 78. (2.00e-): 90.15% LP N₅₂; 0.72% on Si(1); 0.69% on H(3); 3.85% on Ni; 1.20% on C(2).

Orbital 82. (2.00e-): 78.73% LP P₅₅; 4.64% on Si(1); 0.08% on H(3); 7.98% on Ni; 5.67% on C(2).

Orbital 216. (2.00e-): 79.68% 3C Si(1)-H-Ni; 8.98% on Ni(other NAO); 9.76% on C(2).

=====

(5) Spin state study

(NPN)Ni-Cl singlet and triplet: Relative energies, $\Delta(E_e+Disp)$ (kcal/mol)

Triple ζ SMD:

Def2-TZVPP-SDDALL(Ni)	PBE0-D3BJ	ω B97XD-D2*	BP86-D3BJ
S = 0 (singlet)	12.3	13.2	0.0
S = 1 (triplet)	0.0	0.0	6.4

Double ζ gas-phase:

Def2-SVP-SDDALL(Ni)	PBE0-D3BJ	ω B97XD-D2*	BP86-D3BJ
S = 0 (singlet)	12.4	13.7	0.0
S = 1 (triplet)	0.0	0.0	5.5

Single point calculations using geometries optimized with PBE0-D3BJ, Def2-SVP-SDDALL(Ni).

*The long-range corrected functional (ω B97XD) uses a version of Grimme's D2 dispersion model because the D3 model is not implemented.

(NPN)Ni-H singlet and triplet: Relative energies, $\Delta(E_e+Disp)$ (kcal/mol)

Triple ζ SMD:

Def2-TZVPP-SDDALL(Ni)	PBE0-D3BJ	ω B97XD-D2*	BP86-D3BJ
S = 0 (singlet)	4.2	4.6	0.0
S = 1 (triplet)	0.0	0.0	15.9

Double ζ gas-phase:

Def2-SVP-SDDALL(Ni)	PBE0-D3BJ	ω B97XD-D2*	BP86-D3BJ
S = 0 (singlet)	2.3	2.3	0.0
S = 1 (triplet)	0.0	0.0	17.2

Single point calculations using geometries optimized with PBE0-D3BJ, Def2-SVP-SDDALL(Ni).

*The long-range corrected functional (ω B97XD) uses a version of Grimme's D2 dispersion model because the D3 model is not implemented.

(NPN)Ni-SiH₂Ph singlet and triplet $\Delta(E_e+Disp)$ (kcal/mol)

Triple ζ SMD:

Def2-TZVPP-SDDALL(Ni)	PBE0-D3BJ	ω B97XD-D2*	BP86-D3BJ
S = 0 (singlet)	1.4	3.5	0.0
S = 1 (triplet)	0.0	0.0	7.5

Double ζ gas-phase:

Def2-SVP-SDDALL(Ni)	PBE0-D3BJ	ω B97XD-D2*	BP86-D3BJ
S = 0 (singlet)	0.0	9.2	0.0
S = 1 (triplet)	2.4	0.0	23.4

Single point calculations using geometries optimized with PBE0-D3BJ, Def2-SVP-SDDALL(Ni).

*The long-range corrected functional (ω B97XD) uses a version of Grimme's D2 dispersion model because the D3 model is not implemented.

(NPN)Ni-cyclopentene singlet-triplet: Relative energies $\Delta(E_e+Disp)$ in kcal/mol

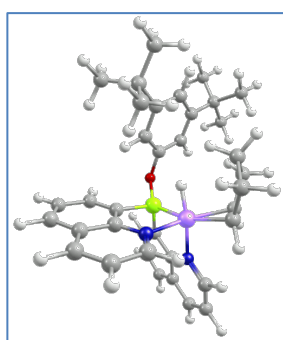
All calculations are PBE0-D3BJ – Double ζ gas-phase:

24 isomeric alkene complexes (including conformers) were considered in both $S = 0$ and $S = 1$ spin states. Seven of them evolved towards isomeric forms of the cyclopentyl intermediate.

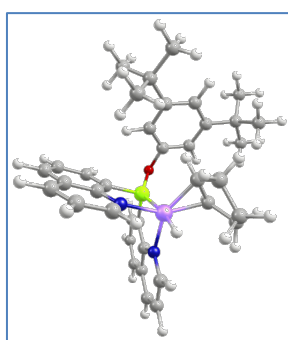
The table below reports selected examples of cyclopentene (**A** and **B**) and cyclopentyl (**C** and **D**) complexes.

Important note: For 22 out of 24 calculated isomers, singlet spin state is more stable than triplet spin state with relative energies similar to those for conformers **A** and **B**). For the two remaining isomers, singlet and triplet spin states are isoenergetic (no more than 0.1 kcal/mol apart).

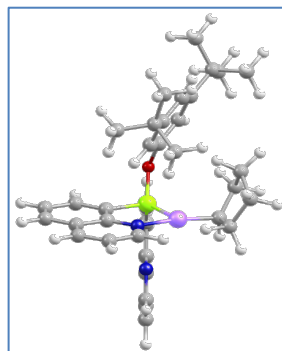
Def2-TZVPP-SDDALL(Ni)	Conformer A	Conformer B	Conformer C	Conformer D
$S = 0$ (singlet)	0.00	4.70	-13.54	-7.81
$S = 1$ (triplet)	10.21	9.60	5.76	16.93



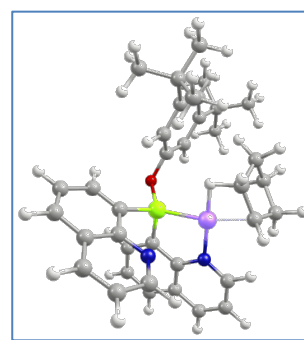
A



B



C



D

In addition, the key transition state for this reaction (addition of the Si-H bond to the Ni-C bond) was found to have a preference for a singlet state.